Compressive Strength Prediction of Self-Compacting Concrete Using Artificial Neural Networks

American Concrete Institute
Always advancing

Concrete Projects Competition 2022

RESEARCH SIGNIFICANCE

Self-compacting concrete is very popular nowadays for self-flowability and self-compaction. It becomes easy to cast at a location where normal concrete cannot be cast. Before using the concrete, it is important to determine the design compressive strength of the concrete. Normally, the strength is determined by using the traditional method, i.e., making a cube or cylindrical specimen and testing the specimen in the laboratory, which is very time-consuming. One has to wait 28 days to get the compressive strength of concrete.

Artificial Neural Network is being used widely in different sector of engineering. In Civil Engineering, ANN also can be used to determine the compressive strength of self-compacting concrete. Once the ANN model is trained using the proper algorithm, the compressive strength of concrete can be predicted without waiting for 28 days or more.

Therefore, this research is conducted to develop an optimum neural network model using the proper algorithm to predict the compressive of self-compacting concrete.

EXECUTIVE SUMMARY

A special type of concrete that flows and consolidates under its weight is called self-compacting concrete. It Is installed without any vibration due to its excellent deformability and flowability. As it is being used in important construction projects nowadays, evaluating its compressive strength is very essential. An artificial neural network (ANN) is predicting tool which can be used to predict output in various sectors. In this study, the compressive strength of industrial waste such as fly ash and silica fume incorporated self-compacting concrete is evaluated at various ages. A nonlinear relationship was used to develop the model relating mix composition and SCC compressive strength. The experimental and expected outcomes were compared with the model prediction to evaluate the predictive capacity, generalize the generated model, and observe suitable matches. The developed ANN network can predict the desired output i.e., compressive strength incorporating industrial waste. Furthermore, the influence of individual parameters viz. cement, silica fume, and fly ash, w/b were also evaluated using parametric analysis. As a result, overall, a higher correlation coefficient of 0.9835with a smaller value of MAPE (0.0347) and RMSE (2.4503) is obtained.

Keywords: ANN; Self-compacting concrete; Artificial Neural Network; Back-propagation; SCC.

TABLE OF CONTENTS

LIST OF FIGURES

LIST OF TABLES

1.1 General

As a material for construction, concrete has been used for more than a century. The material has continued to develop during this time, such as the increased usage of secondary cementitious elements in the binding phase (Heniegal, 2012; Neville, 2011). Due to the self-flow, and self-compaction, SCC is installed without any outward vibration that makes the concrete technology revolutionized (Okamura & Ouchi, 2003; Raheman & Modani, 2013). SCC is different from ordinary concrete in some random cases. Due to its high workability, higher amount of water, and fine content requirement, it has different properties from conventional concrete. Since its development, meaningful improvement was noted in its research and development (Kandasamy & Kothandaraman, 2020; Siddique et al., 2011).

Self-compacting concrete can be produced using industrial waste such as fly ash, ladle slag, silica fume, etc. As fly ash and silica fume give extended durability for the construction project, these are frequently used to produce self-compacting concrete (Deilami et al., 2017; Joshi & Lohtia, 1997; Mazloom et al., 2018). Property enhancement of concrete at different curing states using these industrial byproducts has been documented. Particularly the benefits of long-term water curing are evident (McCarthy et al., 2013). The effect of SCMs on the properties of SCC was studied by several researchers, including, fly ash (Guru Jawahar et al., 2018) and silica fume (Turk et al., 2013a), GGBS (Saini & Vattipalli, 2020). In addition, plastic fibers (Al-Hadithi & Hilal, 2016) and steel fibers (Grünewald & Walraven, 2001) are also used in SCC production. However, the mixing constituents and compressive strength have a non-linear relationship, and there is no theoretical or mathematical relationship between mixture ratio and SCC strength (ACI, 2019; Siddique et al., 2008). As a result, it is necessary to use appropriate methods to predict SCC strength based on the mixing ingredients during the design phase. Artificial Neural Networks (ANN) may be a suitable tool for making this prediction (Taylor, 1992; Yadollahi et al., 2015). From creating examples or data, ANN is a flexible computer method that follows the neural system of a human being. The system is becoming increasingly popular, and it is being used in many engineering fields (Ashteyat & Ismeik, 2018; Taylor, 1992; Ye et al., 2019). Neural network models can predict more specific concrete properties (Hameed et al., 2021) while reducing the experimental work required in the laboratory or

research center and on-site. The primary advantage of the neural network is it does not need any specific equations because it is based only on learning and understanding input-output connections for any complicated problem.

1.2   Research Significance

ANN has been proven by previous studies to be a reliable computer model for predicting concrete strength. It has been demonstrated that an ANN may be utilized to predict the strength of metakaolin-based concrete in a reasonable period and with low error. Compressive strength of SCC at various ages has been predicted utilizing ANN and was shown to be more practicable than classic regression models. Moreover, a neural network has been confirmed as an alternate path for finding out the approximate compressive strength containing fly ash and silica fume. A wide range (15 to 110 MPa) of compressive strengths of SCC, ANN was also utilized to forecast the 'compressive strength' of a regular and high strength SCC, also high-performance concrete including large amounts of fly ash and silica fume. (Serraye et al., 2021).

This study is focused on contributing to developing an ANN model which can accurately forecast the compressive strength of SCC at various ages which contains silica fume and fly ash as partial cement replacement.

1.3   Research Goals

The aim of this research is to predict the strength of self-compacting concrete (SCC) by utilizing an ANN. The objectives of the projects are given below –

➢ To develop an easy-to-use ANN model to predict the compressive strength of SCC containing silica fume and fly ash at different ages.
➢ To evaluate the impact of silica fume, fly ash, and other constituents on the compressive strength of self-compacting concrete.
➢ To investigate the impact of various mix design parameters on the compressive strength of SCC.

CHAPTER 2

LITERATURE REVIEW

2.1 General

SCC, or self-compacting concrete, is a new sort of concrete with, high utility, and large paste volume, and contains cement substitute ingredients like silica fume, slag, fly ash, and pozzolana (Serraye et al., 2021). Cement substitute materials offer various benefits, including lower costs, less use of shared resources, less carbon dioxide emissions, and superior fresh and solidified qualities. In civil engineering, ANN is typically utilized to anticipate the performance of various designing materials, such as compressive strength, mixing constituents, durability, etc. Based on the data from 354 exploratory examinations, an ANN model is constructed for predicting the strength of self-compacting containing fly ash and silica fume by using the back-propagation method along with the Levenberg-Marquardt technique. A nonlinear connection was found between the mix proportion and SCC compressive strength in the model developed.

2.2 Silica fume and Fly-ash based SCC

The heat of hydration is reduced, and durability is increased when cementitious materials are partially replaced with pozzolanic materials like fly ash. Fly ash decreases the necessity of viscosity-modifying agents and improves the slump flow of SCC mixtures. A few scientists have announced that the cementing effectiveness of fly ash will similarly depend upon the level of substitution, fly ash types, and kind of cement utilized. The cementing capacity of fly ash can be considered as 0.5 when the w/b ratios vary between 0.5 and 0.65. Besides, the adequacy of superplasticizer is improved when silica fume is used. Lately, silica fume has been proven to be very effective to produce high-strength, excellent performance concrete. Furthermore, using both a sufficient amount of superplasticizer and silica fume is advantageous since it allows for lower water/binder ratios for a given workability. Because of its reaction with calcium hydroxide framed at the time of cement hydration, silica fume is used as pozzolana which improves the workability of concrete because of its small grain size and durability features, which result in more cementitious materials. The following results may allow the use of significant levels of fly ash, as it is expected that the silica fume's existence will mitigate some of its adverse effects, such as a loss in initial strength.

2.3 Constituent of SCC

2.3.1 Fly ash

Fly ash is a byproduct of power plants burning pulverized coal that produces electricity. Mineral pollutions in coal (quartz, clay, shale and feldspar, quartz) meld together in suspension during combustion and float out with the exhaust gases from the ignition chamber. The interrelated material solidifies and cools as it rises, forming round sparkling particles known as fly ash.

Fly ash reacts synthetically with calcium hydroxide, a result of the chemical interaction between water and cement, to generate additional cementitious materials that increase a variety of appealing qualities of concrete. All the fly ashes exhibit cementitious characteristics to different degrees, depending on the compound and actual properties of both the cement and the fly ash. The material interaction between calcium hydroxide and fly ash is frequently slower than the water and cement, that results in delayed concrete hardening. Two kinds of fly ash are generally utilized in concrete: Class C and Class F. High-calcium fly ashes contain Class C fly ash, with a less than 2% carbon concentration; Class F consists of low-calcium fly ashes with a less than 5% carbon content.
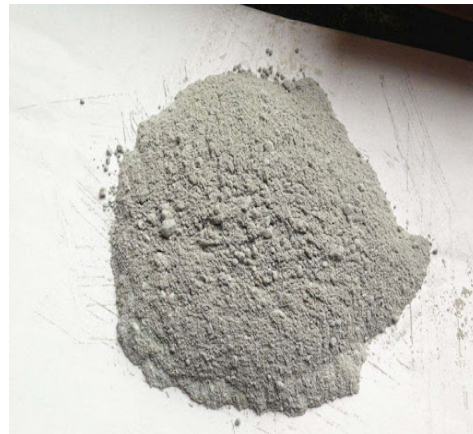
Figure 2-1: Fly ash   Figure 2-2: Silica Fume

2.3.2 Silica fume

Ferrosilicon or silicon metal composites produce silica fume. Probably the most valuable benefit of silica fume is the use of concrete. It is a reactive pozzolan due to its physical and chemical features. Concrete with silica fume has exceptionally high strength and is incredibly long-lasting. Silica fume is available from concrete additive suppliers and is often used during

the concrete manufacturing process once a decision has been made. Placing, restoring, and finishing silica-fume concrete necessitates careful attention on this.

A small portion of silica fume (5 to 15%) can be used as a replacement for cement in concrete. The resulting droop is compensated for by either additional water expansion or the use of superplasticizers. Regardless, compared to the typical concrete mix, there is a substantial improvement in compressive strength. This is particularly true when superplasticizers are used. Similarly, silica fume can be used as a halfway replacement for concrete. Although the cementitious materials' weight remains the same, the limited fineness of silica fume causes an increase in water demand.

2.4　ANN in Civil Engineering

ANN is a prediction tool that is widely used nowadays to predict desired output and different sectors. In civil engineering, ANN can be used very effectively. It learns from experimental or analytical/theoretical data. These types of models are capable of classifying data, predicting values, and assisting in decision-making analogous to a response surface technique. Compared to traditional numerical analysis processes (e.g., regression analysis), a trained ANN can produce more trustworthy findings with far less processing work. (Asteris & Kolovos, 2019; Hornik et al., 1989).

ANN functions similarly to the human brain's organic neural network (Hinton et al., 2006; Schmidhuber, 2015). The artificial neurons are the most fundamental component of a neural network. Like biological neurons, inputs are provided to the artificial neuron, which produces an output after processing it using a mathematical function. Weights are assigned to input parameters before the data reaches the neuron to replicate the biological neuron's unpredictable nature.

The ANN capability has been developed for a variety of structural engineering applications. Previously the various properties of concrete such as creep, shear strength, etc. were predicted utilizing ANN. (Asteris, Armaghani, et al., 2019; Hodhod et al., 2018). The technique was similarly applied to determine the cement-based mortar's strength (Asteris, Apostolopoulou, et al., 2019). Neural network modeling was also utilized to predict the tensile strength of SCC (Mazloom & Yoosefi, 2013). In addition, ANNs have been used to monitor the structural health of civil infrastructures (Ye et al., 2019) and durability (Kellouche et al., 2021).

2.5 Advantages of ANN

There are numerous benefits of artificial neural networks. Some of them are given below:

1. Neural networks have the ability to self-learn and create output that is not limited by the input.
2. Data loss has no impact on the system's functionality because the data is maintained in its networks instead of a database.
3. Artificial neural networks may learn from past occurrences and use what they've learned in the future when a similar circumstance arises, allowing them to handle real-time situations.
4. It is used in situations where a rapid assessment of learned objective capability is necessary.
5. Even if a neuron fails to react or a piece of data is absent, the network can recognize the problem and provide the desired result.

3.1 General

The goal of this study is to use ANN to evaluate the compressive strength of SCC. The examination used a variety of worldwide standard methodologies. The materials utilized in this investigation will be described in this chapter. The material properties and mix design are obtained from the literature.

3.2 Materials

Cement (Ordinary Portland Cement), silica fume, fly ash, aggregates, superplasticizer, viscosity modifying agent, and water are generally used to produce SCC. The study evaluated the performance of SCC influenced by the concrete parameters using ANN.

3.2.1 Cement

For getting ready the concrete mixture the Ordinary Portland Cement (OPC) is utilized. Ordinary Portland Cement's usual composition is shown in Table 3-2, and its actual characteristics are presented in Table 3-1.

Table 3-2: Typical cement composition

Components	CEM-I
Clinker	95 – 100%
Gypsum	0 – 5%

Table 3-1: Properties of cement

Properties	Results
Soundness	Sound
Fineness	$> 4000 \text{ cm}^2/\text{gm}$
Specific gravity	3.15
Initial setting time	1 hour 5 minutes
Final setting time	3 hour 20 minutes

Figure 3-1: Ordinary Portland Cement

3.2.2 Aggregate

The characteristics of fine and coarse aggregate are shown in Table 3-5 and Table 3-3. A typical grading scheme for coarse aggregate is presented in Table 3-4. Fine and coarse aggregates are shown in Figure 3-3.

Table 3-5: Properties of fine aggregate

Properties	Value
Specific gravity	2.60
Absorption capacity	1.8%
Fineness modulus	2.90
Unit weight	1620 kg/m^3

Table 3-3: Properties of coarse aggregate

Properties	Value
Specific gravity	2.71
Absorption capacity	1.0%
Fineness modulus	N/A
Unit weight	1563 kg/m^3

Table 3-4: Grading of coarse aggregate

Sieve size (mm)	% Passing	% Retain
12.5	100	0
9.5	45	55
4.75	0	45

Figure 3-3(a): Fine aggregate

Figure 3-3(b): Coarse aggregate

3.2.3 Fly ash

Fly ash was used partially as a cement substitute. The chemical and physical characteristics of fly ash defined by *ASTM C618* are given in Table 3-6 & Table 3-7. Typical fly ash is shown in Figure 2-1.

Table 3-6: Physical properties of fly ash

Properties	Results
Colour	Blackish gray
Specific gravity	2.13
Blaine Fineness	619 m^2/kg

Table 3-7: Chemical composition of fly ash (*ASTM C618*)

Constituents	% by weight
Loss on ignition	4.17
Silica (SiO_2)	58.55
Iron Oxide (Fe_2O_3)	3.44
Alumina (Al_2O_3)	28.20
Calcium Oxide (CaO)	2.23
Magnesium Oxide (MgO)	0.32
Total Sulphur (SO_3)	0.07
Insoluble residue	–
Alkalis; (a) Sodium Oxide (Na_2O)	0.58
(b) Potassium Oxide (K_2O)	1.26

3.2.4 Silica fume

Silica fume has also been used to replace cement in some cases. Table 3-8 lists the chemical and physical characteristics of silica fume as determined by. In Figure 2-2, standard silica fume is shown.

Table 3-8: Chemical and physical properties of typical silica fume (ASTM Cl240)

Properties	Value
Specific gravity	2.2
Mean grain size (μm)	0.15
Specific area (cm^2/gm)	150000 – 300000
Color	Light to dark gray
Silicon dioxide (SiO_2)	85
Aluminum oxide (Al_2O_3)	1.12
Iron oxide (Fe_2O_3)	1.46
Calcium oxide (CaO)	0.2 – 0.8
Magnesium oxide (MgO)	0.2 – 0.8
Sodium oxide (Na_2O)	0.5 – 1.2
Potassium oxide (K_2O)	0.5 – 1.2
Loss on ignition	< 6.0

3.2.5 Superplasticizer

Plasticizers and superplasticizers delay the curing of concrete. Their use in concrete or mortar permits a decrease in the water/binder ratio without affecting the mixture's workability, allowing self-compacting and premium concrete production. Table 3-9 shows the standard physical and chemical characteristics of superplasticizers according to *ASTM C494 / C494M*.

Table 3-9 Physical and Chemical properties of Superplasticizer (ASTM C494)

Properties	Values
Appearance	Light yellow or no color
Specific Gravity	1.1 ± 0.02
Viscosity	22 at 20°C
Chloride content	< 0.2 %
Chemical base	Polycarboxylic either
pH	7 ± 1
Relative density	1.09 ± 0.01 at 25°C
Solid content	Not less than 30% by weight

3.2.6   Viscosity Modifying Agent

Viscosity modifying agents (VMA) can be used to improve the protection from segregation and bleeding. Their use, just on the other hand, allows for a change in mortar and concrete rheology and stream characteristics. This feature may be used to simplify a variety of concrete types. As a safety net, a small amount of VMA may be used in some of the SCC mixes to account for the unexpected group-to-clump variations in water content, which may easily transform stable blends into separated and dismissed loads (Benaicha et al., 2015; Leemann & Winnefeld, 2007).

3.2.7   Mixing water

Non-consumable water can be utilized for mixing and curing if the source does not contrarily affect the concrete properties. Tap water was used for the blending of concrete.

RESEARCH METHODOLOGY

4.1 General

For the strength prediction of SCC using an Artificial neural network, a lot of reliable data/information of mix design and compressive strength is required. The more the accurate date, the more the reliable prediction is. The test data/information was obtained from available literature and in-house experimental results. These were then used to build this network model.
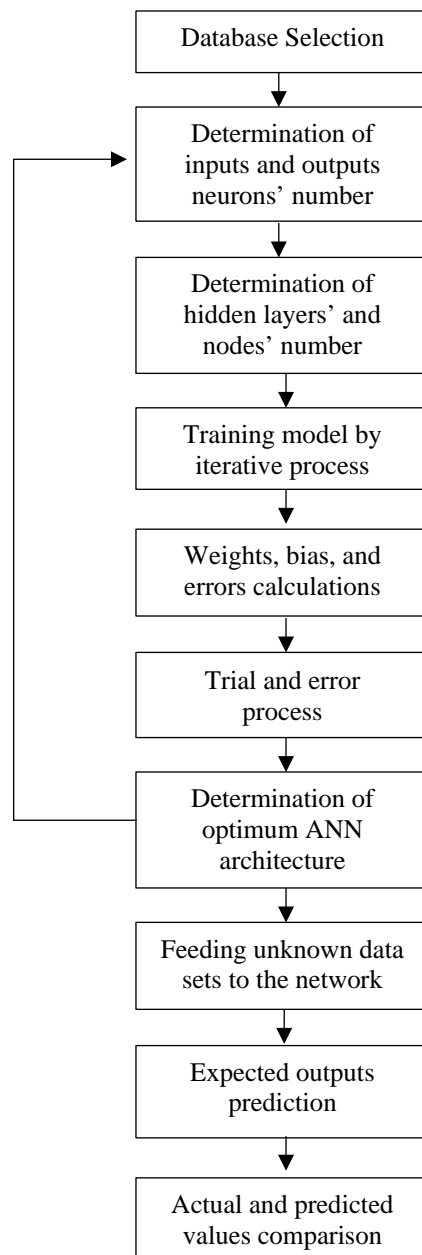
Figure 4-1: Work flow of the whole process

The development cycle of this model was separated into three primary segments. The central focus is on gathering and analyzing data on SCC which contains fly ash and silica fume only. The second section focused on determining various training parameters such as execution duration, performance function, and learning method as well as appropriate neural network models. Finally, the proposed ANN models were approved, and their performances were checked in the third and final phase, which included a comparison with other available test data. A flow diagram of the overall process is given in Figure 4-1.

4.2 Architecture of ANN

A back-propagation neural network is a multilayer, feed-forward (Hinton et al., 2006) network in which data transmits from the input to the output layer, with no back loops and nodes in the layers that make up the same layer, are not linked to each other. However, they are connected to all nodes in the preceding and next layers. The basic structure (Asteris & Kolovos, 2019) of a BPNN can be written as –

$$N - H_i - H_{i+1} - H_{i+2} - \ldots - H_{NHL} - M \qquad (4\text{-}1)$$
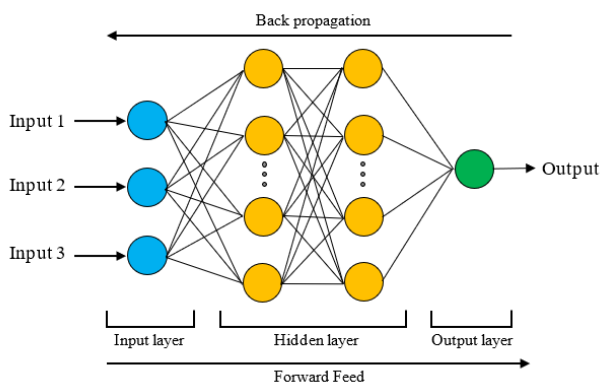
Figure 4-2: A 3-5-5-1 BPNN model structure
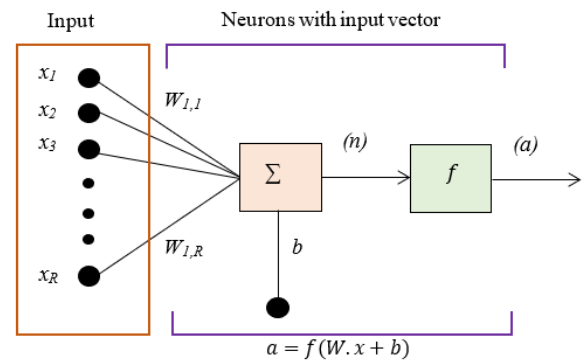
Figure 4-3: ANN model with a single hidden layer

Where, H_i denotes the number of nodes in the i_{th} hidden layer for $i = 1, 2, \ldots \ldots, NHL$, N represents the number of input neurons. M is the number of output neurons, and NHL is the number of hidden layers. Figure 4-2 shows a BPNN with three neurons in the input layer, two hidden layers with six neurons each, and one neuron in the output layer referred to as a 3-6-6-1 BPNN.

Although researchers regularly suggest multilayer NN models, it should be emphasized that the models only with a single hidden layer have the ability to reliably predict any prediction challenge. In Figure 4-3, A representation of a single hidden layer neuron is shown.

Every member inputs $x_1,...,$ x_R is multiplied by the correlating weights $w_{i, 1},...,$ $w_{i, R}$ for each neuron x, and the values of weight are delivered to the summation function's junction, which generates the dot product *(W.x)* of the weight vector $W = [w_{i,1},..., w_{i,R}]$ and the input vector $x = [x_1,..., x_R]^T$. The net input n, is formed by adding the bias b to the dot product.

$$n = W.x = W_{i,1}x_1 + W_{i,2}x_2 + \cdots + W_{i,R}x_R + b \qquad (4\text{-}2)$$

The ANN's complexity and performance may be influenced significantly by the transfer (or activation) function selected. Although sigmoidal activation or transfer functions are the most popular, other functions can also be employed. Various activation functions have been offered in previous studies (Lecun et al., 2015; Schmidhuber, 2015). The combined hyperbolic tangent sigmoid transfer function – 'tansig' and linear transfer function – 'purelin' were found to be suitable for the problem under consideration in this research. The training data is delivered into the network during the training stage, which attempts to map the input and output values. The weights are adjusted to obtain this mapping by reducing the following error function –

$$E = \sum (y_i - x_i)^2 \qquad (4\text{-}3)$$

Where y_i and x_i represent the network's exact value and forecast value, respectively. The optimization training method plays a critical part in creating a high-quality mapping, and a thorough analysis was conducted to determine the best fit for this challenge. Back-propagation technique is the most widely used method, as the name implies, in which data/information is sent backward to the network to change the weights and reduce the error function. An approach called gradient descent is utilized to correctly modify the weights, which calculates the gradients of the cost function,

However, there is no reliable method for determining a network's ideal architecture prior to training. The concealed layers, on the other hand, must contain a minimal number of nodes. This is because the network may memorize the training data if there are too many hidden nodes.

The ANN would be unable to successfully interpolate between neighboring training data points in such circumstances. The network's ability to create an adequate relationship between input and output variables will be limited if there are too few hidden nodes (Anderson & McNeil, 1992). Typically, the number of hidden layers and nodes is determined through trial and error.

4.3 Dealing with Overfitting

An obvious difficulty that emerges during the training stage of a network is overfitting. The network has done an excellent job of learning the provided training data at this point (the error function has very tiny), but when additional data is added to this network, the error increases dramatically. The prediction of the network is unsatisfactory. Numerous algorithms and techniques for deciding the optimum number of hidden nodes along with the hidden layers have been presented to avoid overfitting. Additionally, the training of the ANNs may be stopped before it has a chance to fully understand the data, and a normalization term may be introduced to the transfer function to smooth out the mapping (Asteris, Kolovos, et al., 2016; Boger & Guterman, 1997; Chen, 2013; Giovanis & Papadopoulos, 2015).
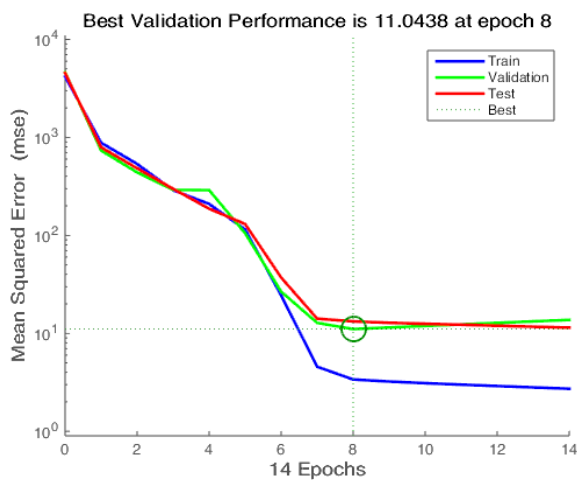
Figure 4-4: Performance of the proposed model
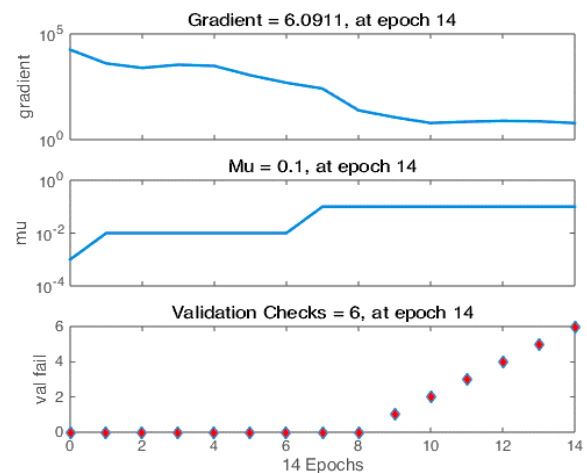
Figure 4-5: Training state of the proposed model

Another dataset was utilized to verify the developed model to prevent over-fitting the neural network model to the data during iterative training. When the error for the validation set starts to rise, training is terminated. The training in this article ends at epoch 8, which has an MSE of 11.043 (MATLAB). Figure 4-4 illustrates that when the validation test is simulated using the derived model, the error in the validation test increases after epoch 8.

A check for validation was performed from the beginning of epoch 0 to after each epoch, as shown in Figure 4-5. The training was ended since the MSE increased in 8 consecutive epochs, and the algorithm picked which epoch had the lowest MSE.

4.4   Experimental Database

An extensive and trustworthy dataset is required for any artificial neural network to function properly. A comprehensive range of experimental data was necessary to determine the connection between the mixing elements of self-compacting concrete and its observed characteristics. It is hard for a single researcher to generate enough experimental data to train ANN fully. Another difficulty is the accuracy of accessible data because the database trains the optimal developed network; hence, the trained network will fail to predict proper values if the data or information is misleading. Only a tiny group of inaccurate data can damage a larger volume of data. Table A-1 of Appendix-I shows the dataset that has been utilized in the proposed ANN model. The whole data is organized into nine input parameters (silica fume, fly ash and cement content, w/b ratio, coarse aggregates, fine aggregates, viscosity modifying agent (VMA), superplasticizer, and age of testing). The single output variable is the compressive strength of SCC.

A database of 354 mixtures was collected from the literature, all of which had similar physical and chemical characteristics. The requirements for data identification were defined by the omission of a few SCC characteristics in some literature and the uncertainty of testing procedures and combination proportions. The values acquired experimentally were compared to the predicted results produced by the neural network. A pair of input vectors and output vectors were utilized for training the ANN. The input vector contained mixing variables in the network model, and the output vector had only one element, compressive strength.

Most previous studies created databases based on their experimental results, restricting the results to their immediate environment; however, our database was created using various data sources, including literature from multiple countries, and it can be used in a broader range of situations. Table 4-1 shows the boundary values of variables used to develop the model. Table 4-2 shows the range of these input and output variables and how they are distributed.

Table 4-1 Input and output ranges

Constituents	Minimum	Maximum	Average
Input variables			
Water/binder	0.3	0.45	0.37
Cement (kg/m^3)	135	600	356.94
Fly ash (kg/m^3)	0	420	124.97
Silica fume (kg/m^3)	0	150	22.61
Fine aggregates (kg/m^3)	657	1166	908.46
Coarse aggregates (kg/m^3)	590	1000	731.27
Superplasticizer (kg/m^3)	0.585	13.8	5.31
VMA (kg/m^3)	0	4.03	0.1
Age (days)	7	180	40.92
Output variable			
Compressive strength (MPa)	17.7	106.6	56.47

Table 4-2 Distribution of inputs variables in the database

W/B		Cement		Fly ash	
Range (kg/m^3)	Ferq.	Range (kg/m^3)	Ferq.	Range (kg/m^3)	Ferq.
0.25-0.31	42	100-250	91	0-115	183
0.32-0.38	160	251-400	128	116-230	87
0.39-0.44	120	401-550	119	231-345	69
0.45-0.5	32	551-700	16	346-460	15

Silica fume		Fine aggregates		Coarse aggregates	
Range (kg/m^3)	Ferq.	Range (kg/m^3)	Ferq.	Range (kg/m^3)	Ferq.
0-40	261	650-790	78	550-675	171
41-80	78	791-930	107	676-800	68
81-120	92	931-1070	135	801-925	97
121-160	1	1071-1200	34	926-1050	18

Superplasticizer		VMA		Ages	
Range (kg/m^3)	Ferq.	Range (kg/m^3)	Ferq.	Range (days)	Ferq.
0.5-3.87	159	0-1.125	348	7	91
3.88-7.25	64	1.126-2.25	0	28	170
7.26-10.63	104	2.251-3.375	0	90	85
10.64-14	27	3.376-4.5	6	180	8

4.5　Normalization of the Data

The most important stage is considered to be the normalization of data for any type of challenge in the area of software-based computational approaches, i.e., artificial neural network strategies. This stage is a pre-processing stage. During this pre-processing stage of this investigation, the Min-Max normalization techniques were utilized (Delen et al., 2006). The Min-Max normalization approach was used to equalize the nine input variables (Table 4-1) and one output variable. According to Iruansi et al. (Iruansi et al., 2012), data must be normalized within the range indicated by suitable minimum and maximum limits values of the related variable to prevent issues related to poor learning rates of the network. The input and output variables were normalized using the equation (4-4), within the range [0.10, 0.90] in this study.

$$x_{norm} = \frac{x - min(x)}{max(x) - min(x)} \qquad (4\text{-}4)$$

Where, x_{norm} is the normalized value for the given data x.

4.6　Development of Model

4.6.1　Determination of input neurons

The variables that impact concrete strength are used to calculate the number of input neurons. As there are too many factors, it is impossible to create the training architecture in a reasonable amount of time, which is also impractical in the view of an engineering strategy that permits for a ±10% error margin. During the early development stage, all conceivable variables are considered. 9 variables (fly ash, silica fume, w/b, cement, coarse aggregate, fine aggregate, superplasticizer, viscosity modifying agent, curing age) are considered to be fundamental input neurons in the proposed model (Figure 4-6).

4.6.2　Determination of output neurons

With time, the concrete's strength increases. The compressive strength after 28 days is a good indicator of design quality and control. The initial strength of concrete within 7 days after placing is critical in determining if the concrete can handle disposal and shoring reduction. The concrete strength is measured at four distinct ages. The basic number of output neurons is considered to be one neuron and utilized for the proposed model since we are interested in determining the compressive strength of SCC as an output.
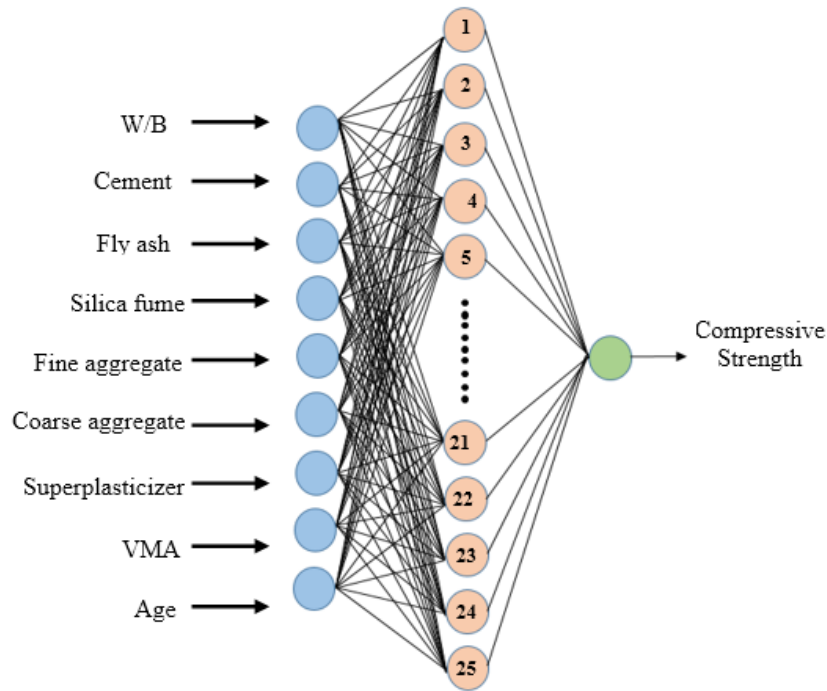
Figure 4-6 Visual representation of the developed model

4.7   Training algorithms

4.7.1   General

The different optimization methods were investigated, to determine the optimum training algorithm. These methods include the one-step secant, quasi-newton, gradient descent, and Levenberg-Marquardt. All of the ANNs under investigation have been tested using all of the training techniques described above. The Levenberg-Marquardt method (implemented by levmar), offered by far the best ANN prediction of the output parameter among these algorithms. This technique appears to be best for training feedforward back propagation neural networks with nonlinear issues that are moderately large (up to several hundred neurons per layer) (Lourakis, 2005).

It is worth mentioning that the Levenberg–Marquardt algorithm differs significantly from the other methods (Lourakis, 2005). In addition to nonlinear problems, this technique seems to be the quickest for training feed-forward neural networks of a reasonable size (weights ranging from a few hundred to a few thousand). It is also well-implemented in the MATLAB software. Because the MATLAB environment has the built-in function to solve the matrix equation, hence its capabilities are improved.

27

4.7.2   Determination of ANN parameters

Several distinct BPNN models were designed and deployed in this study. The model was trained using 248 mix data out of a total of 354 data pairs (70% of total data points) and was validated and tested using the remaining 107 data pairs (30% of the total pairs). More precisely, 53 data pairs (15%) were used to validate the trained model, and 53 data pairs (15%) were used for testing the model. The ANNs' architecture includes a hidden layer with 5 to 30 neurons.. (Apostolopoulou et al., 2019; Armaghani et al., 2019; Asteris, Tsaris, et al., 2016; Cavaleri et al., 2017; Nikoo et al., 2017). The maximum allowable error is calculated by the rule described in the previous literature (Lee et al., 2001; Lee & Han, 2002).

$$y = tansig\,(x) = \frac{e^x - e^{-x}}{e^x + e^{-x}} = \frac{2}{1 + e^{-2x}} - 1 \qquad (4\text{-}5)$$

$$y = purelin\,(x) = x \qquad (4\text{-}6)$$

Equations (4-5) and (4-6) specify the transfer or activation function utilized in the training of the neural network model, which is a 'tansig' and a 'purelin' function. The output of the 'tansig' function ranges from +1 to -1.
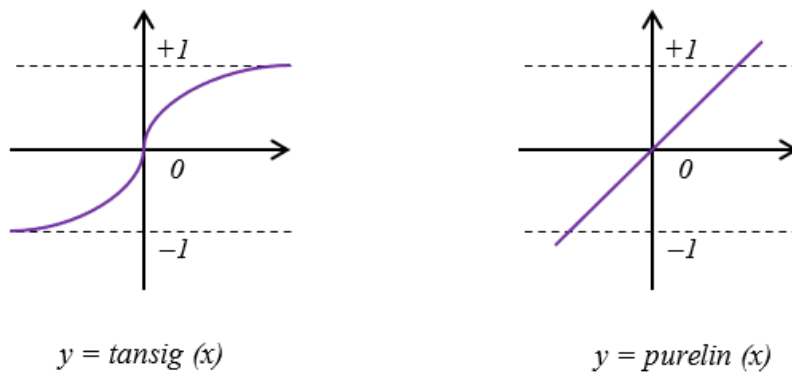
Figure 4-7 Sigmoidal transfer function — tansig and purelin

Table 4-4 summarizes the parameters that were employed in the ANN training. To compare the predictions generated by the neural network, the datasets are divided into three sets – training sets, validation sets, and testing sets. The data points are divided into three groups at random in the majority of the cases.

Table 4-3 Training parameters of the developed BBNN model

Training parameters	Values
Training algorithm	Levenberg-Marquardt
Normalization	Min-Max (0.1-0.9)
No. of input neurons	9
No. of hidden layers	1
No. of neurons in hidden layer	25
No. of output neurons	1
Training goal	0
Performance function	MSE
Transfer function	Tansig & Purelin
Time	Infinite
Learning cycle	1000
Minimum gradient	1×10^{-7}
Maximum fail	6

MSE: Mean square error
Tansig: Hyperbolic tangent sigmoid transfer function
Purelin: Linear transfer function

4.8   Model Validation

The capacity of a well-trained neural network model to extrapolate the predictions in addition to the training data and to operate reliably when given unexpected, unknown data ranging from the input variable's range utilized during training is what determines its validity. Consequently, the developed ANN model's capacity to reliably predict the self-compacting concrete characteristics of new data gathered from other researchers who were not included in the training datasets must be evaluated. The more data there is, the more accurate an ANN forecast of SCC characteristics will be.

The SCC's strength had to be predicted by the developed model associated with each combination of values within the nine critical factors from a total of 16 unseen data (Liu, 2010; Naik et al., 2012; Turk et al., 2013a; Zhu & Bartos, 2003). Table 5-1 shows validation of new data records and comparison of predicted values using the optimum developed neural network model. The calculated relative percentage error in every prediction in Table 5-1 is calculated by Eqn. (4-7).

$$E(\%) = \left| \frac{O_{actual} - O_{predicted}}{O_{actual}} \right| \times 100 \qquad (4\text{-}7)$$

Where, O_{actual} is the actual output and $O_{predicted}$ is the predicted output generated by the developed neural network model.

The model validation is expressed as a total relative percentage error, which demonstrates that the developed model can reliably predict SCC compressive strength at various ages.

4.9 Performance of the model

There are several statistical indexes that are used to assess the performance of the neural network model. The network models developed in this paper were evaluated using three statistical indexes – Root mean square error (RMSE), Mean absolute percentage error (MAPE), and Pearson correlation coefficient (R^2). These parameters are widely used and accepted (Chugh, n.d.; Vandeput, n.d.). Smaller RMSE and MAPE indicate more exact predictions. Higher R^2 values indicate that the analytical and projected values are more correlated. The following formulas were used to determine the statistical parameters (Results given in Table 4-6) stated above (Apostolopoulou et al., 2019) –

$$RMSE = \sqrt{\frac{1}{n}\sum_{i=1}^{n}(y_i - x_i)^2} \qquad (4\text{-}8)$$

$$MAPE = \frac{1}{n}\sum_{i=1}^{n}\left| \frac{y_i - x_i}{y_i} \right| \qquad (4\text{-}9)$$

$$R^2 = 1 - \left(\frac{\sum_{i=1}^{n}(y_i - x_i)^2}{\sum_{i=1}^{n}(y_i - \bar{y})^2} \right) \qquad (4\text{-}10)$$

Where, y_i and x_i denote the actual and forecasted values respectively, and n denotes the total number of datasets.

4.10 Optimum proposed BPNN model

Various BPNN (back-propagation neural network) models have been created and examined to identify the best model for predicting self-compacting concrete compressive strength. In particular, 26 distinct ANN architectures have been developed based on the usage of one hidden layer.

Table 4-4 Statistical indexes of the optimum BPNN models

SL No.	BPNN Model	Dataset	R^2	RMSE
20	9-24-1	Training	0.9807	3.135283
		Validation	0.8913	6.315061
		Test	0.9514	4.871345
21	9-25-1	Training	0.9912	1.746425
		Validation	0.9629	3.32265
		Test	0.9631	3.321144
22	9-26-1	Training	0.9823	2.57682
		Validation	0.9178	5.872819
		Test	0.9456	4.382921
23	9-27-1	Training	0.9922	1.723369
		Validation	0.9301	4.721229
		Test	0.9432	4.521062
24	9-28-1	Training	0.9948	1.403567
		Validation	0.9351	5.161395
		Test	0.9345	4.737088
25	9-29-1	Training	0.9851	2.336664
		Validation	0.9456	4.844585
		Test	0.9008	5.54617
26	9-30-1	Training	0.9872	2.142429
		Validation	0.9359	5.216321
		Test	0.9044	5.488169

Table 4-5 shows seven cases of ANN models that have been developed. Appendix-II contains other cases of optimal BPNN models. The optimal BPNN model 9-25-1 is chosen based on the R^2, and RMSE values for the compressive strength prediction. The chosen model 9-25-1 refers to a neural network architecture consisting of nine input variables, one hidden layer with 25 nodes, and one output neuron. The values of the statistical indexes R^2, MAPE, and RMSE of the best proposed BPNN are shown in Table 4-6.

Table 4-5 Coefficients of the optimum proposed neural network model.

ANN model	R^2	MAPE	RMSE
9-25-1	0.9835	0.0347	2.4503

R^2: Pearson Correlation Coefficient
MAPE: Mean Absolute Percentage Error
RMSE: Root Mean Square Error
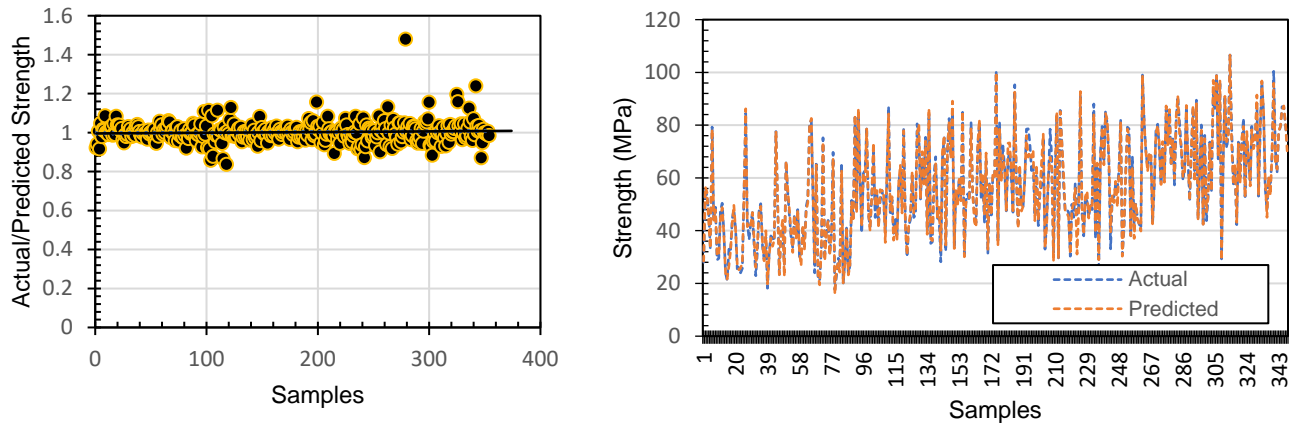
Figure 4-8 Actual vs predicted strength for the test dataset

Figure 5-1 shows a comparison between the actual values and predicted values of the best BPNN model for all ages. It is clearly demonstrated that he suggested optimal 9-25-1 model correctly forecasts the SCC's compressive strength. It's worth mentioning that the variation of every sample utilized in the testing procedure is less than ±10%. (Figure 5-1). The two graphs in Figure 4-8 show the same conclusion, with experimental values compared to the suggested optimal 9-25-1 NN model's equivalent values for test datasets.

As a result, the final model (Table 4-1) has nine input parameters, one hidden layer with 25 hidden neurons, tansig and purelin as activation functions, and one output variable that is the SCC's compressive strength.

5.1 General

The final goal of this research project is to develop the optimum neural network model and to establish a tool for practical uses. The developed model can be accepted if the model can predict the output effectively. The output of the dataset utilized in this investigation is checked via cross-validation. Cross-validation is a way of determining how accurate a developed model is. The input data pair is separated into multiple groups each used to evaluate a model that fits the remaining portion.

Statistical approaches are frequently employed to create empirical relationships between numerous interacting elements. The process is usually complicated and convoluted, especially when dealing with nonlinear relations. The critical parameters must also be known to create the statistical model. On the other hand, backpropagation neural networks have a more straightforward modeling procedure since no mathematical equation is required for the input and output variables. ANNs help to study systems with many variables and identify patterns and features that were previously unknown. The neural networks are taught to handle noisy or imprecise data since they are trained on actual test data. The model may easily be updated when new data becomes available by retraining using the latest data patterns.

For the strength prediction of industrial waste incorporated SCC, various BPNN models were created and evaluated. In particular, 26 distinct ANN architectures have been developed based on the usage of one hidden layer. Table 4-5 shows indexes of six ANN model cases that have been developed. The optimal BPNN model 9-25-1 is chosen based on the R^2, and RMSE values for the compressive strength prediction. The chosen model 9-25-1 refers to a neural network architecture that has nine input variables and one output variable respectively, as well as one hidden layer with 25 nodes. The values of the statistical indexes R^2, MAPE, and RMSE of the best proposed BPNN are listed in Table 4-6.

For the comparison of actual values and predicted output by the best BPNN model, two graphs are plotted, as shown in Figure 4-8. It is clear that, within a small error margin, the suggested optimal 9-25-1 model can correctly forecast the industrial waste incorporated SCC's

compressive strength. It is worth noting that the variation of almost every sample utilized in the testing procedure is less than ±10%. (Figure 5-1).

The following figures show the actual and predicted strength to compare the model's performance. Figure 5-1 depicts the overall performance of the ANN, forecasting the strength in all ages. Figure 5-2 to Figure 5-5 shows the strength prediction performance at 7, 28, 90, and 180-day periods. The results indicate that most points are within the ±10% lines, implying that the networks may accurately predict SCC strength. The overall correlation coefficient of the model obtained was 0.9835, which is very high and a smaller RMSE value of 2.4503 compared to other similar studies (Nguyen et al., 2020; Uysal & Tanyildizi, 2011).

The final trained model recalled data that had not been used at the training phase (354 mixes) to evaluate the accuracy of the ANN model. A total of 16 unknown combinations were presented to the developed model within the training data sets range to predict the output, i.e., SCC strength. Table 5-1 shows the proportion of mixtures (kg/m^3), as well as the measured and predicted values.
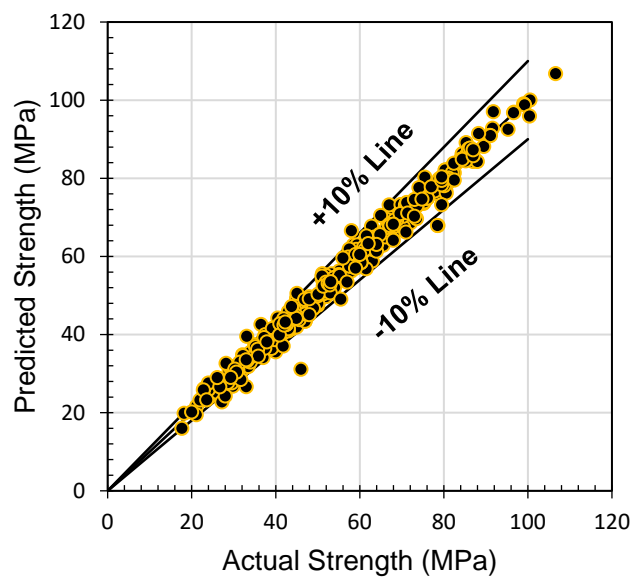
Figure 5-1: Actual v/s predicted strength for all ages
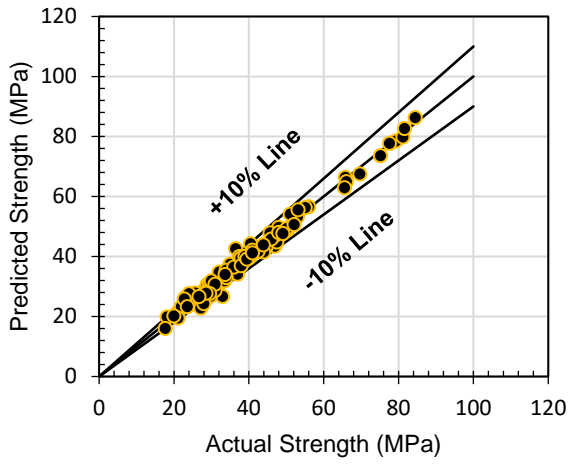
Figure 5-2. Actual v/s predicted strength for 7-days.
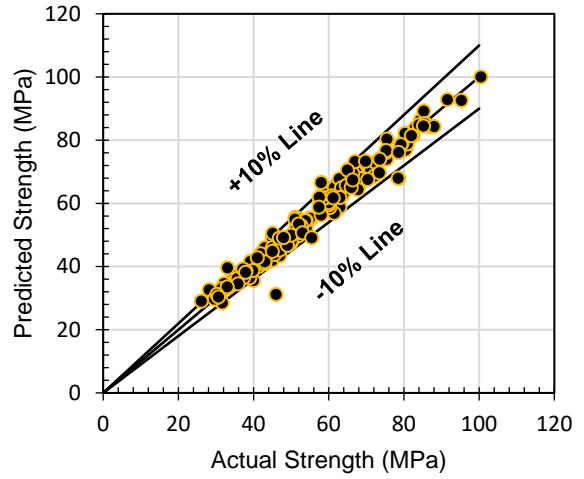
Figure 5-3. Actual v/s predicted strength for 28-days.
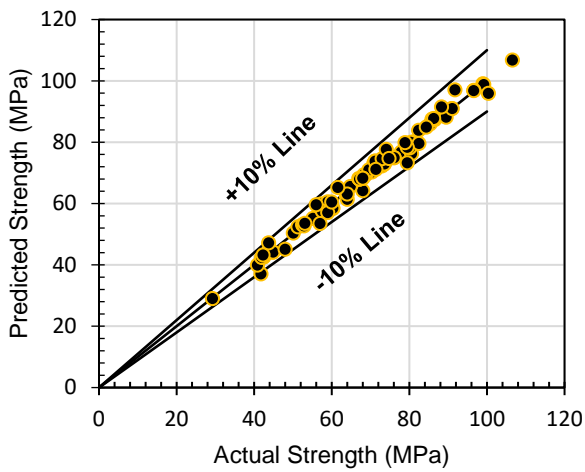
Figure 5-4. Actual v/s predicted strength for 90-days.
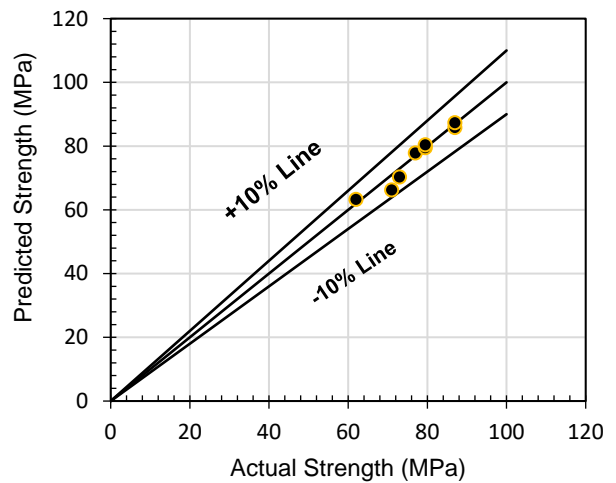
Figure 5-5. Actual v/s predicted strength for 180-days.

Table 5-1: Actual and predicted strength (MPa) for testing data sets of ANN

									Output		
				Input variables							
W/B	Cement	Fly Ash	Silica fume	Fine agg.	Coarse agg.	SP	VMA	Age	Actual Strength	Predicted Strength	E(%)
0.30	620	0	0	740	775	8.06	4.03	7	47.1	46.33	1.63
0.31	589	0	31	740	775	8.06	4.03	7	56.5	56.52	0.03
0.31	573	0	47	740	775	8.06	4.03	7	60.1	60.27	0.28
0.30	620	0	0	740	775	8.06	4.03	28	60.2	60.72	0.87
0.31	589	0	31	740	775	8.06	4.03	28	73.1	72.63	0.64
0.31	573	0	47	740	775	8.06	4.03	28	76.3	77.46	1.53
0.35	154	309	51	980	621	2.056	0	7	40.5	40.06	1.09
0.32	220	247.5	82.5	685	880	8.89	0	90	68.3	69.32	1.50
0.39	220	180	0	916	900	1.4	0	28	45	46.69	3.76
0.30	540	0	60	1059	595	8.58	0	7	84.5	86.21	2.03
0.40	600	0	0	810	660	13.8	0.9	7	35	37.35	6.70
0.35	206	257	51	1001	621	2.57	0	7	48.2	47.97	0.47
0.35	327	173	0	902	803	4.42	0	28	61.6	61.16	0.71
0.45	371	159	0	768	668	0.86	0.082	28	41.4	40.01	3.35
0.40	510	0	90	810	660	13.8	0.9	28	55.3	55.06	0.44
0.40	428	0	23	1157	640	8.569	0	28	75.3	76.70	1.86

SP: Superplasticizer
VMA: Viscosity Modifying Agent
E(%): Relative percentage error

5.2 Parametric Analysis of Developed ANN Model

Parametric analysis of a model can be defined as a technique for identifying whether alterations in the input assumptions influence the output of the model (Grady, 2014). It is important to know the impact of input variables on the output variable. By parametric analysis, it is possible to know how much sensitive the input variables are. This offers feedback on the input variables that are more important and less. Furthermore, by deleting the inconsequential variables, the input space can be decreased, resulting in a reduction in the complication of the network and the necessary time for training. Therefore, a parametric analysis was conducted in this study to test the sensitivity of the input parameters to the output parameter i.e., SCC strength.

This has been done by analyzing the effect of altering one parameter while keeping all others constant. Some key input variables were assessed for this purpose. As a result, functional relationships between the mixture variables and the compressive strength are established.

5.2.1 Effect of fly ash content

To evaluate the fly ash that how much it is sensitive to the compressive strength, fly ash was altered in different amounts with different cement content while keeping other parameters constant. In Figure 5-6, the impact of fly ash with different cement content is shown. The replacement level of fly ash has a considerable impact on the strength.

Increasing the fly ash level with the increasing amount of cement content increased the compressive strength (28-day) until the optimum amount of fly ash and then decreased the strength. The increased amount of fly ash after the optimum level as a cement replacement has a direct relationship with the reduction in strength. Similar results have been found in previously published studies (Ahmad et al., 2020; Naik et al., 2012).

The pozzolanic reaction of alumino-silicate oxides in fly ash with calcium hydroxide generates additional cementitious compounds. As a result, concrete containing fly ash gains strength over time. However, in general, the total cement and fly ash content over 550 kg/m3 was found an optimum range of total binder. Beyond this, the cement content replaces the fine aggregate, which interferes with the water demand and packing of the matrix (Chandra & Bendapudi, 2015)

5.2.2 Effect of Silica fume content

Silica fume has a considerable impact on the strength of SCC. For the evaluation of the silica fume impact on the strength, the amount of silica fume was altered while other parameters were kept constant. The compressive strength (28-day) increases with the increasing amount of silica fume. Figure 5-7 shows the strength variation with varying amounts of silica fume replacement (from 0 to 130 kg) and different cement content. Previous studies also show the result (Turk et al., 2013a).

This is because silica fume is a very active and fine mineral additive. In concrete, it enhances the bond between fine aggregate and the hydrated cement in the mix within a short period as the material is very fine. In addition, the unreacted material fills the very fine pores in the matrix (Abdi Moghadam & Izadifard, 2019). All these mechanisms increase the compressive strength of SCC.
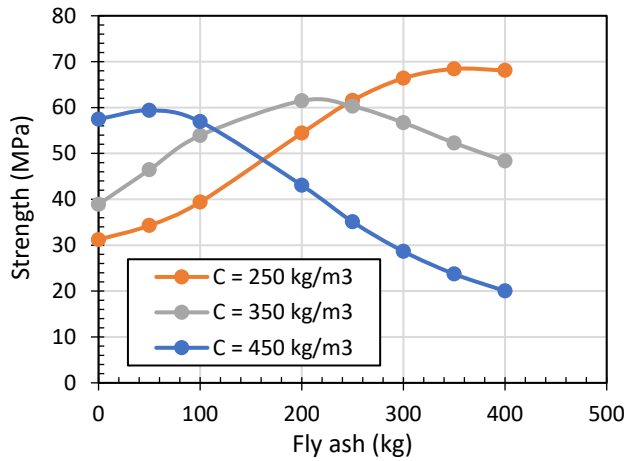
Figure 5-6 Impact of fly ash on strength.
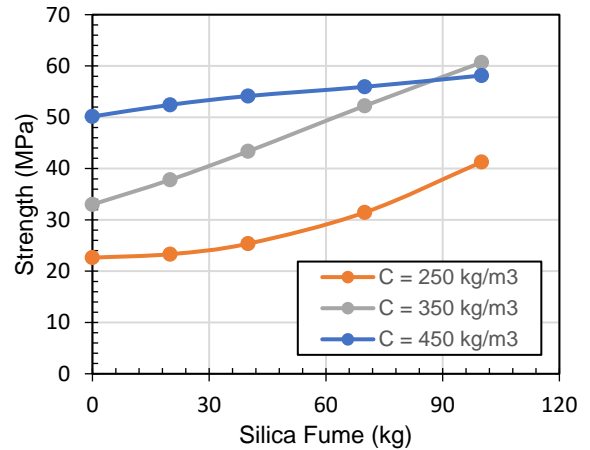
Figure 5-7 Silica fume impact on SCC strength.

5.2.3 *Effect of w/b ratio*

Water-binder ratio is one of the most important parameters for any kind of concrete. The compressive strength has a direct relationship with the w/b ratio. This was notably true when making highly workable self-compacting concrete with a large amount of paste, frequently resulting in a greater w/b ratio (Neville, 2011). Figure 5-8 shows the strength change concerning the w/b ratio for varying amounts of fly ash after 28 days. The combined effects of the increasing amount of fly ash and w/b ratio reduce the strength after the optimum fly ash level at 28 days. Siddique (Siddique, 2011) also reported this phenomenon in their earlier study.

The strength of concrete depends on its porosity. The hydration reaction requires a minimum amount of water. On the other side, more water (increased w/b ratio) causes the dilution of cement paste and increases the water-filled pore space between the particles (Beaudoin & Odler, 2019). Hydrates must grow larger to fill the gap space between them to interact and improve strength. In short, any extra water beyond the hydration requirement will produce more capillary pores, reducing the area of solid hydrates for the same cross-sectional area of concrete and lowering the strength. Sometimes, with a lower w/b ratio, desirable workability can be achieved by using a superplasticizer. However, the use of too much superplasticizer may affect the ultimate strength (Islam et al., 2019).
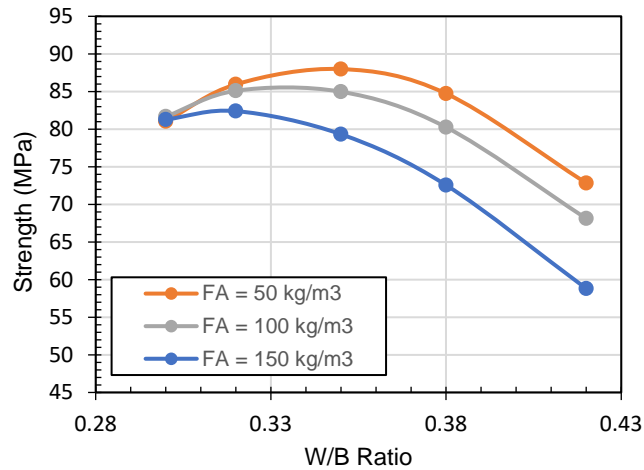
Figure 5-8 Effect of w/b ratio

5.2.4   Effect of Superplasticizer

Superplasticizer is critical for improving the rheological characteristics of SCC. Therefore, it is a necessary component for the production of SCC. Figure 5-9 shows the change in strength with varying SP dosages (4 to 12 kg) with the varying amounts of fly ash (50 to 150 kg) at 28 days.

With the increase of FA and superplasticizer, the strength of SCC at 28 days decreases. For a given flowability, the superplasticizer can enhance strength by reducing mixed water or lowering both water and cement content to reach the desired flowability and strength (Aïtcin, 1995). The production of self-compacting concrete only with Portland cement, and fly ash causes the lower amount of superplasticizer requirement to achieve equivalent strength (Naik et al., 2012). However, the mechanism of superplasticizer with cement and the same with fly ash does not work similarly. Increasing superplasticizer content based on total cementitious binder would negatively impact the strength. A minor difference was noted with a change in fly ash content.

The situation was different with silica fume. Figure 5-10 shows the change in 28-day compressive strength with various SP dosages (from 4 to 12 kg) for different silica fume concentrations. As the finest material, silica fume generally demands more water (Levy, 2012). Increased superplasticizer content may improve the situation with low water content, especially when using a higher amount of silica fume in the matrix. Furthermore, increasing the

superplasticizer concentration beyond an optimum level may negatively influence the 28-day strength (Neville, 2011).

The decrease in strength after the optimum doses of SP is due to more water for concrete mixing since the addition of a superplasticizer. An increased amount of superplasticizer results in bleeding and segregation, affecting concrete's cohesiveness and homogeneity, resulting in the SCC strength decreases (Ben Aicha, 2020).
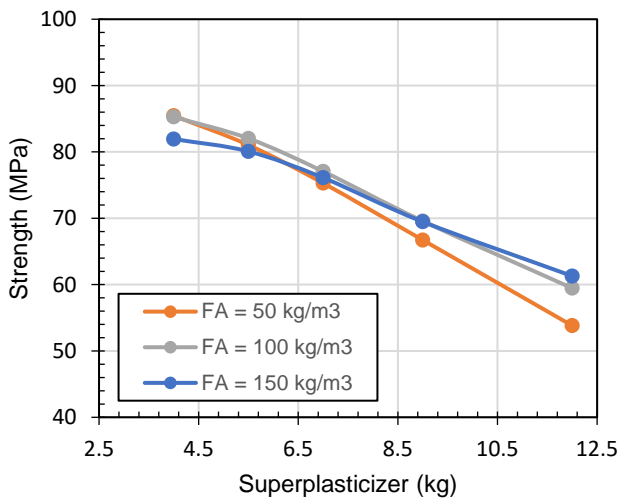
Figure 5-9. Effect of SP with fly ash.
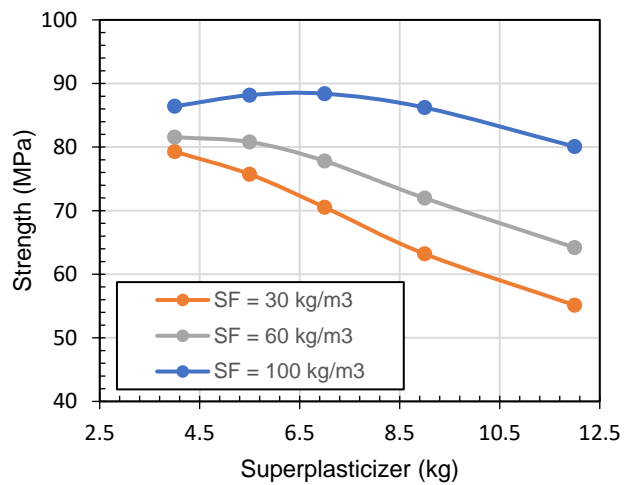
Figure 5-10. Effect of SP with silica fume.

5.3   Weights and bias of the developed ANN model

There is a common tendency of the researchers that they only describe the structure of the optimum neural network model without providing the final weights and bias values. This is not a good practice that any design that does not deliver these benefits is of little utility to other researchers and practicing engineers. On the contrary, if a suggested neural network structure is associated with weights and bias values, it may be beneficial as it allows the developed model to be easily implemented, making it available to anybody enthusiastic about simulating challenges.

In light of this, the weights and bias for both the hidden layer and output layer of the optimum developed model, are presented in Table 5-2. These values will be used to reliably predict the SCC compressive strength based on optimum ANN architecture by using the characteristics of the model.

Table 5-2 Weights and bias of the developed ANN model

BPNN 9-25-1											
IW {1,1} (25x9)									LW {2,1}T (1x25)	B {1,1} (25x1)	B {2,1} (1x1)
0.3861	-0.4473	0.4919	0.0274	0.8131	1.3142	0.1048	1.2833	-1.5875	0.9962	-1.6549	-0.6427
1.0395	-0.2965	-0.2982	-0.4424	0.5316	1.1786	0.1352	0.9777	0.4948	-1.4051	-1.7453	
-0.2321	-0.2157	-0.4404	0.1140	-1.0337	1.0060	0.9061	-0.7301	1.5175	-0.4738	1.8990	
-0.2823	0.4689	-0.7107	-0.0478	-1.4016	-1.1022	-1.0172	0.1878	0.7796	-0.7083	1.7008	
0.7149	-1.6305	-1.2778	-0.3979	-0.9373	0.4673	0.9046	0.1710	-0.5227	-1.0667	-1.9707	
0.9685	-0.7779	1.1270	-0.1479	1.9167	0.1299	-1.5541	1.7196	-0.2594	-0.4856	-1.8697	
1.9281	0.2177	0.0759	-0.4684	-1.3793	1.3550	1.5138	0.7255	0.3946	0.8545	-1.0466	
-0.1691	1.4644	-0.4006	0.3072	-1.8379	-0.9159	0.6371	-0.5948	1.0737	0.2871	1.0449	
0.3091	-0.7747	0.3626	0.0331	-0.3506	-0.6753	1.0043	-0.0761	1.1456	0.5239	1.5515	
0.6127	-1.4309	-0.5610	-1.6405	-1.9280	-0.4206	0.6837	-0.5580	0.2822	0.3924	1.3449	
0.7234	0.9496	0.7862	0.1525	0.4599	-0.5193	-0.1344	0.1630	-2.1063	-0.7570	-1.0688	
0.8253	-1.2847	-1.0034	-0.6834	0.5478	0.6240	0.6328	0.0740	-1.8104	-0.0328	-0.4352	
0.2207	-0.8225	-1.1234	-0.1373	-0.6733	-1.1219	-0.2812	1.9193	-2.3166	0.8236	-0.1502	
0.3545	1.0817	0.3916	-1.1905	-0.7781	0.2309	0.2823	-0.9864	-1.4884	-0.2995	0.4903	
-0.2682	-0.2869	0.2464	0.7185	0.8875	0.9881	1.8874	-2.2981	-0.6912	-0.1886	0.0859	
-0.2798	0.9279	-1.5636	1.1721	0.4103	-0.7516	0.6479	0.7328	1.3019	0.1447	0.2141	
0.6581	0.8694	1.1364	-0.0470	-1.6680	-0.6695	0.1035	-0.4887	-0.3012	-0.6475	-0.8591	
-0.6016	-2.1822	-1.1098	-0.7833	0.5695	0.6940	1.0854	1.4069	-1.3123	-0.5593	-1.1375	
0.4914	-1.6347	-1.3426	-1.1195	-1.8386	2.4454	0.6347	-1.6106	-0.2362	-1.3057	1.7809	
-1.3700	0.5219	-0.5910	0.3400	0.5876	1.2926	-1.4310	-0.7877	1.5973	-0.1393	-0.8487	
0.3590	0.6764	0.1044	0.0669	0.1056	-1.7477	0.6490	0.4066	1.0818	-0.5243	1.8353	
-2.5806	1.4288	-0.3096	0.1330	-2.1023	-1.0061	0.3953	0.4119	0.0472	-0.2485	-1.9827	
1.0294	-0.2437	0.7336	0.0214	1.9664	-1.2201	-0.2390	-0.8424	-0.5995	-0.5984	1.4398	
0.5215	-1.2627	0.0068	0.0489	-0.3049	-0.8894	0.5640	-1.1179	-0.6934	0.8124	1.6658	
0.1507	-0.1606	-0.7280	-0.7205	-0.4271	0.0389	1.1528	-0.5212	1.6653	0.5405	1.5548	

IW {1,1} = Values of weight matrix between input and hidden layer

LW {2,1} = Values of weight matrix between hidden and output layer

B {1,1} = Values of bias of the hidden layer

B {2,1} = Values of bias of the output layer

CHAPTER 6

CONCLUSIONS AND RECOMMENDATION

6.1   General

The main goal of the paper was to develop an optimum BPNN model and to develop a procedure to create a tool or program for practical uses. Following the goal, a network architecture is developed which can reliably predict the strength of SCC. Also, proposed an approach to creating a spreadsheet program for practical users. This spreadsheet can be very handy in the practical field. The following conclusion can be drawn from the research study –

a)   The proposed neural network architecture can make a reliable prediction as the trained network obtained very low RMSE (2.4503) and MAPE (0.0347) values. Also, the higher R^2 (0.9835) value is obtained making the predicted values very similar to actual values.

b)   Using parametric analysis, the developed network can assess the sensitivity or influence of individual parameters. The impact of individual parameters on compressive of SCC was significant. The sensitivity result agrees with the previously published studies.

c)   Although the model prediction is limited to its boundary limits (ranges of input parameters), it can be easily retrained with a broader scope by utilizing the proposed optimum neural network model.

6.2   Limitations

Few limitations are observed for this proposed ANN model. These are listed in the following:

- Only if the researcher or practitioner knows all of the experimental values for all of the input variables utilized in this study, then the proposed ANN model can be applied.
- It is essential to note that the developed ANN model may be used with reliability for the variable values ranging between the minimum and maximum limits (as shown in Table 4-1); else, the projected value may not be as good as expected.
- The proposed model is restricted to SCC with SF and fly ash. More investigation is required to determine the influence of ladle slag, metakaolin, and fiber-reinforced, etc., in SCC, as well as the workability of the material.

- Sometimes the input values outside the range, especially the zero value of the binder can lead to negative output values.

6.3   Recommendations for future study

Researchers have a lot of opportunities to study more about SCC through ANN. Some of them can be listed as follows:

- As the developed ANN model is restricted to SCC with silica fume and fly ash, further research is required to evaluate the effect of other constituents such as metakaolin, ladle slag, polypropylene fiber, etc. in the self-compacting concrete.
- The V-funnel time, J-Ring test result, the L-box ratio, Slump flow, etc., of the SCC can also be investigated by the ANN prediction model.
- Elasticity modulus, water permeability, oxygen permeability, as well as durability of SCC with silica fume and fly ash can be investigated through ANN model development.
- The effect of SCC in high temperatures can also be studied by the ANN model.
- ANN model can be built up for zero values of the binder.

Abdi Moghadam, M., & Izadifard, R. A. (2019). Experimental investigation on the effect of silica fume and zeolite on mechanical and durability properties of concrete at high temperatures. *SN Applied Sciences 2019 1:7*, *1*(7), 1–11. https://doi.org/10.1007/S42452-019-0739-2

ACI. (2019). *ACI PRC-237-07 Self-Consolidating Concrete* (p. 30). American Concrete Institute.

Ahmad, J., Ihsan, M. T., Manan, A., Zaid, O., Ullah, R., & Abbas, G. (2020). *Evaluating the Effect of Fly Ash on the Rheological and Mechanical Performance Self-Compacted Concrete*. *10*.

Aïtcin, P. C. (1995). Developments in the application of high-performance concretes. *Construction and Building Materials*, *9*(1), 13–17. https://doi.org/10.1016/0950-0618(95)92855-B

Al-Hadithi, A. I., & Hilal, N. N. (2016). The possibility of enhancing some properties of self-compacting concrete by adding waste plastic fibers. *Journal of Building Engineering*, *8*, 20–28. https://doi.org/10.1016/j.jobe.2016.06.011

Anderson, D., & McNeil, G. (1992). Artificial neural networks technology for neutron spectrometry and dosimetry. *Radiation Protection Dosimetry*, *126*(1–4), 408–412. https://doi.org/10.1093/rpd/ncm084

Apostolopoulou, M., Armaghani, D. J., Bakolas, A., Douvika, M. G., Moropoulou, A., & Asteris, P. G. (2019). Compressive strength of natural hydraulic lime mortars using soft computing techniques. *Procedia Structural Integrity*, *17*, 914–923. https://doi.org/10.1016/j.prostr.2019.08.122

Armaghani, D. J., Hatzigeorgiou, G. D., Karamani, C., Skentou, A., Zoumpoulaki, I., & Asteris, P. G. (2019). Soft computing-based techniques for concrete beams shear strength. *Procedia Structural Integrity*, *17*, 924–933. https://doi.org/10.1016/j.prostr.2019.08.123

Ashteyat, A. M., & Ismeik, M. (2018). Predicting residual compressive strength of self-compacted concrete under various temperatures and relative humidity conditions by artificial neural networks. *Computers and Concrete*, *21*(1), 47. https://doi.org/10.12989/CAC.2018.21.1.047

Asteris, P. G., Apostolopoulou, M., Skentou, A. D., & Moropoulou, A. (2019). Application of artificial neural networks for the prediction of the compressive strength of cement-based mortars. *Computers and Concrete*, *24*(4), 329. https://doi.org/10.12989/CAC.2019.24.4.329

Asteris, P. G., Armaghani, D. J., Hatzigeorgiou, G. D., Karayannis, C. G., & Pilakoutas, K. (2019). Predicting the shear strength of reinforced concrete beams using Artificial Neural Networks. *Computers and Concrete*, *24*(5), 469. https://doi.org/10.12989/CAC.2019.24.5.469

Asteris, P. G., & Kolovos, K. G. (2019). Self-compacting concrete strength prediction using surrogate models. *Neural Computing and Applications*, *31*, 409–424. https://doi.org/10.1007/s00521-017-3007-7

Asteris, P. G., Kolovos, K. G., Douvika, M. G., & Roinos, K. (2016). Prediction of self-compacting concrete strength using artificial neural networks. *European Journal of Environmental and Civil Engineering*, *20*, s102–s122. https://doi.org/10.1080/19648189.2016.1246693

Asteris, P. G., Tsaris, A. K., Cavaleri, L., Repapis, C. C., Papalou, A., Di Trapani, F., & Karypidis, D. F. (2016). Prediction of the fundamental period of infilled rc frame structures using artificial neural networks. *Computational Intelligence and Neuroscience*, *2016*. https://doi.org/10.1155/2016/5104907

ASTM C1240 - 20 Standard Specification for Silica Fume Used in Cementitious Mixtures. (n.d.). Retrieved July 24, 2021, from https://www.astm.org/Standards/C1240

ASTM C494 / C494M - 19 Standard Specification for Chemical Admixtures for Concrete. (n.d.). Retrieved July 24, 2021, from https://www.astm.org/Standards/C494

ASTM C618 - 19 Standard Specification for Coal Fly Ash and Raw or Calcined Natural Pozzolan for Use in Concrete. (n.d.). Retrieved July 24, 2021, from https://www.astm.org/Standards/C618.htm

Beaudoin, J., & Odler, I. (2019). Hydration, Setting and Hardening of Portland Cement. *Lea's Chemistry of Cement and Concrete*, 157–250. https://doi.org/10.1016/B978-0-08-100773-0.00005-8

Behfarnia, K., & Farshadfar, O. (2013). The effects of pozzolanic binders and polypropylene fibers on durability of SCC to magnesium sulfate attack. *Construction and Building Materials*, *38*, 64–71. https://doi.org/10.1016/j.conbuildmat.2012.08.035

Ben Aicha, M. (2020). The superplasticizer effect on the rheological and mechanical properties of self-compacting concrete. *New Materials in Civil Engineering*, 315–331. https://doi.org/10.1016/B978-0-12-818961-0.00008-9

Benaicha, M., Roguiez, X., Jalbaud, O., Burtschell, Y., & Alaoui, A. H. (2015). Influence of silica fume and viscosity modifying agent on the mechanical and rheological behavior of self compacting concrete. *Construction and Building Materials*, *84*, 103–110. https://doi.org/10.1016/j.conbuildmat.2015.03.061

Bingöl, A. F., & Tohumcu, I. (2013). Effects of different curing regimes on the compressive strength properties of self compacting concrete incorporating fly ash and silica fume. *Materials and Design*, *51*, 12–18. https://doi.org/10.1016/j.matdes.2013.03.106

Boger, Z., & Guterman, H. (1997). Knowledge extraction from artificial neural networks models. *Proceedings of the IEEE International Conference on Systems, Man and Cybernetics*, *4*, 3030–3035. https://doi.org/10.1109/icsmc.1997.633051

Bui, V. K., Akkaya, Y., & Shah, S. P. (2002). Rheological model for self-consolidating

concrete. *ACI Materials Journal*, *99*(6), 549–559. https://doi.org/10.14359/12364

Cavaleri, L., Chatzarakis, G. E., Di Trapani, F. D., Douvika, M. G., Roinos, K., Vaxevanidis, N. M., & Asteris, P. G. (2017). Modeling of surface roughness in electro-discharge machining using artificial neural networks. *Advances in Materials Research (South Korea)*, *6*(2), 169–184. https://doi.org/10.12989/amr.2017.6.2.169

Chandra, S., & Bendapudi, K. (2015). Contribution of Fly ash to the properties of Mortar and Concrete. *International Journal of Earth Sciences and Engineering*, *04*(October 2011), 1017–1023.

Chen, Z. (2013). An overview of bayesian methods for neural spike train analysis. In *Computational Intelligence and Neuroscience* (Vol. 2013). https://doi.org/10.1155/2013/251905

Choudhary, R., Gupta, R., & Nagar, R. (2020). Impact on fresh, mechanical, and microstructural properties of high strength self-compacting concrete by marble cutting slurry waste, fly ash, and silica fume. *Construction and Building Materials*, *239*, 117888. https://doi.org/10.1016/j.conbuildmat.2019.117888

Chugh, A. (n.d.). *MAE, MSE, RMSE, Coefficient of Determination, Adjusted R Squared — Which Metric is Better?* Retrieved August 29, 2021, from https://medium.com/analytics-vidhya/mae-mse-rmse-coefficient-of-determination-adjusted-r-squared-which-metric-is-better-cd0326a5697e

Deilami, S., Aslani, F., & Elchalakani, M. (2017). Durability assessment of self-compacting concrete with fly ash. *Computers and Concrete*, *19*(5), 489. https://doi.org/10.12989/CAC.2017.19.5.489

Delen, D., Sharda, R., & Bessonov, M. (2006). Identifying significant predictors of injury severity in traffic accidents using a series of artificial neural networks. *Accident Analysis and Prevention*, *38*(3), 434–444. https://doi.org/10.1016/j.aap.2005.06.024

Dhiyaneshwaran, S., Ramanathan, P., Baskar, I., & Venkatasubramani, R. (2013). Study on durability characteristics of self-compacting concrete with fly ash. *Jordan Journal of Civil Engineering*, *7*(3), 342–353.

Faez, A., Sayari, A., & Manie, S. (2020). Mechanical and Rheological Properties of Self-Compacting Concrete Containing Al2O3 Nanoparticles and Silica Fume. *Iranian Journal of Science and Technology - Transactions of Civil Engineering*, *44*(2015), 217–227. https://doi.org/10.1007/s40996-019-00339-y

Gesoğlu, M., Güneyisi, E., & Özbay, E. (2009). Properties of self-compacting concretes made with binary, ternary, and quaternary cementitious blends of fly ash, blast furnace slag, and silica fume. *Construction and Building Materials*, *23*(5), 1847–1854. https://doi.org/10.1016/j.conbuildmat.2008.09.015

Gesoğlu, M., & Özbay, E. (2007). Effects of mineral admixtures on fresh and hardened properties of self-compacting concretes: Binary, ternary and quaternary systems. *Materials and Structures/Materiaux et Constructions*, *40*(9), 923–937. https://doi.org/10.1617/s11527-007-

9242-0

Gholhaki, M., kheyroddin, A., Hajforoush, M., & Kazemi, M. (2018). An investigation on the fresh and hardened properties of self-compacting concrete incorporating magnetic water with various pozzolanic materials. *Construction and Building Materials*, *158*, 173–180. https://doi.org/10.1016/j.conbuildmat.2017.09.135

Giovanis, D. G., & Papadopoulos, V. (2015). Spectral representation-based neural network assisted stochastic structural mechanics. *Engineering Structures*, *84*, 382–394. https://doi.org/10.1016/j.engstruct.2014.11.044

Grady, J. O. (2014). System Requirements Analysis: Second Edition. *System Requirements Analysis: Second Edition*, 1–803. https://doi.org/10.1016/C2012-0-06079-6

Grünewald, S., & Walraven, J. C. (2001). Parameter-study on the influence of steel fibers and coarse aggregate content on the fresh properties of self-compacting concrete. *Cement and Concrete Research*, *31*(12), 1793–1798. https://doi.org/10.1016/S0008-8846(01)00555-5

Güneyisi, E., Gesolu, M., & Özbay, E. (2010). Strength and drying shrinkage properties of self-compacting concretes incorporating multi-system blended mineral admixtures. *Construction and Building Materials*, *24*(10), 1878–1887. https://doi.org/10.1016/j.conbuildmat.2010.04.015

Güneyisi, E., Gesoɩlu, M., Booya, E., & Mermerdaş, K. (2015). Strength and permeability properties of self-compacting concrete with cold bonded fly ash lightweight aggregate. *Construction and Building Materials*, *74*, 17–24. https://doi.org/10.1016/j.conbuildmat.2014.10.032

Guru Jawahar, J., Yakshareddy, B., Sashidhar, C., Sreenivasulu, C., & Ramana Reddy, I. V. (2018). Evolution of 112-day drying shrinkage equation of fly ash blended self-compacting concrete. *Asian Journal of Civil Engineering*, *19*(6), 703–712. https://doi.org/10.1007/S42107-018-0054-Z

Hameed, M. M., AlOmar, M. K., Baniya, W. J., & AlSaadi, M. A. (2021). Incorporation of artificial neural network with principal component analysis and cross-validation technique to predict high-performance concrete compressive strength. *Asian Journal of Civil Engineering 2021 22:6*, *22*(6), 1019–1031. https://doi.org/10.1007/S42107-021-00362-3

Heniegal, A. M. (2012). Numerical Analysis for Predicting of Self Compacting Concrete Mixtures Using Artificial Neural Networks. *JES. Journal of Engineering Sciences*, *40*(6), 1575–1597. https://doi.org/10.21608/jesaun.2012.114530

Hinton, G. E., Osindero, S., & Teh, Y. W. (2006). A fast learning algorithm for deep belief nets. *Neural Computation*, *18*(7), 1527–1554. https://doi.org/10.1162/neco.2006.18.7.1527

Hodhod, O. A., Said, T. E., & Ataya, A. M. (2018). Prediction of creep in concrete using genetic programming hybridized with ANN. *Computers and Concrete*, *21*(5), 513. https://doi.org/10.12989/CAC.2018.21.5.513

Hornik, K., Stinchcombe, M., & White, H. (1989). Multilayer feedforward networks are

universal approximators. *Neural Networks*, *2*(5), 359–366. https://doi.org/10.1016/0893-6080(89)90020-8

Iruansi, O., Guadagnini, M., Pilakoutas, K., & Neocleous, K. (2012). Predicting the shear resistance of RC beams without shear reinforcement using a Bayesian neural network. *International Journal of Reliability and Safety*, *6*(1–3), 82–109. https://doi.org/10.1504/IJRS.2012.044299

Islam, G. M. S., Raihan, M. T. M. T., Hasan, M. M., & Rashadin, M. (2019). Effect of retarding superplasticizers on the properties of cement paste, mortar and concrete. *Asian Journal of Civil Engineering*, *20*(4), 591–601. https://doi.org/10.1007/s42107-019-00128-y

Joshi, R. C., & Lohtia, R. P. (1997). *Fly ash in concrete, production, properties and uses. Advances in Concrete technology* (Volume 2). Gordon and Breach Science Publishers.

Kandasamy, S., & Kothandaraman, S. (2020). The effect of formwork liner on the service life of self-compacting concrete. *Asian Journal of Civil Engineering*, *21*(7), 1239–1247. https://doi.org/10.1007/S42107-020-00272-W

Kellouche, Y., Boukhatem, B., Ghrici, M., Rebouh, R., & Zidol, A. (2021). Neural network model for predicting the carbonation depth of slag concrete. *Asian Journal of Civil Engineering*, *22*(7), 1401–1414. https://doi.org/10.1007/S42107-021-00390-Z

Khodabakhshian, A., de Brito, J., Ghalehnovi, M., & Asadi Shamsabadi, E. (2018). Mechanical, environmental and economic performance of structural concrete containing silica fume and marble industry waste powder. *Construction and Building Materials*, *169*(2018), 237–251. https://doi.org/10.1016/j.conbuildmat.2018.02.192

Lecun, Y., Bengio, Y., & Hinton, G. (2015). Deep learning. In *Nature* (Vol. 521, Issue 7553, pp. 436–444). Nature Publishing Group. https://doi.org/10.1038/nature14539

Lee, S. C., & Han, S. W. (2002). Neural-network-based models for generating artificial earthquakes and response spectra. *Computers and Structures*, *80*(20–21), 1627–1638. https://doi.org/10.1016/S0045-7949(02)00112-8

Lee, S. C., Park, S. K., & Lee, B. H. (2001). Development of the approximate analytical model for the stub-girder system using neural networks. *Computers and Structures*, *79*(10), 1013–1025. https://doi.org/10.1016/S0045-7949(00)00199-1

Leemann, A., & Winnefeld, F. (2007). The effect of viscosity modifying agents on mortar and concrete. *Cement and Concrete Composites*, *29*(5), 341–349. https://doi.org/10.1016/J.CEMCONCOMP.2007.01.004

Levy, S. M. (2012). Calculations Relating to Concrete and Masonry. *Construction Calculations Manual*, 211–264. https://doi.org/10.1016/B978-0-12-382243-7.00005-X

Liu, M. (2010). Self-compacting concrete with different levels of pulverized fuel ash. *Construction and Building Materials*, *24*(7), 1245–1252. https://doi.org/10.1016/j.conbuildmat.2009.12.012

Lourakis, M. I. a. (2005). A Brief Description of the Levenberg-Marquardt Algorithm Implemened by levmar. *Matrix*, *3*(January 2005), 2. http://www.ics.forth.gr/~lourakis/

Mazloom, M., Soltani, A., Karamloo, M., Hassanloo, A., & Ranjbar, A. (2018). Effects of silica fume, superplasticizer dosage and type of superplasticizer on the properties of normal and self-compacting concrete. *Advances in Materials Research*, *7*(1), 45. https://doi.org/10.12989/AMR.2018.7.1.045

Mazloom, M., & Yoosefi, M. M. (2013). Predicting the indirect tensile strength of self-compacting concrete using artificial neural networks. *Computers and Concrete*, *12*(3), 285. https://doi.org/10.12989/CAC.2013.12.3.285

McCarthy, M. J., Islam, G. M. S., Csetenyi, L. J., & Jones, M. R. (2013). Evaluating Test Methods for Rapidly Assessing Fly Ash Reactivity for Use in Concrete. *World of Coal Ash Conference, April 22-25*.

Naik, T. R., Kumar, R., Ramme, B. W., & Canpolat, F. (2012). Development of high-strength, economical self-consolidating concrete. *Construction and Building Materials*, *30*, 463–469. https://doi.org/10.1016/j.conbuildmat.2011.12.025

Neville. (2011). *Properties of Concrete* (5th ed.). Pearson Education Limited.

Nguyen, T. T., Pham Duy, H., Pham Thanh, T., & Vu, H. H. (2020). Compressive Strength Evaluation of Fiber-Reinforced High-Strength Self-Compacting Concrete with Artificial Intelligence. *Advances in Civil Engineering*, *2020*. https://doi.org/10.1155/2020/3012139

Nikoo, M., Sadowski, Ł., Khademi, F., & Nikoo, M. (2017). Determination of Damage in Reinforced Concrete Frames with Shear Walls Using Self-Organizing Feature Map. *Applied Computational Intelligence and Soft Computing*, *2017*. https://doi.org/10.1155/2017/3508189

Okamura, H., & Ouchi, M. (2003). Self-Compacting Concrete. *Journal of Advanced Concrete Technology*, *1*(1), 5–15. https://doi.org/10.3151/jact.1.5

Patel, R., Hossain, K. M. A., Shehata, M., Bouzoubaâ, N., & Lachemi, M. (2004). Development of statistical models for mixture design of high-volume fly ash self-consolidating concrete. *ACI Materials Journal*, *101*(4), 294–302. https://doi.org/10.14359/13363

Prajapati Krishnapal, R. (2013). Rheological Characteristics of Self Compacting Concrete Containing Flyash -. *International Journal of Current Research and Review*, *5*(10), 137.

Raheman, A., & Modani, P. P. O. (2013). *Prediction of Properties of Self Compacting Concrete Using Artificial Neural Network*. *3*(4), 333–339.

Sabet, F. A., Libre, N. A., & Shekarchi, M. (2013). Mechanical and durability properties of self consolidating high performance concrete incorporating natural zeolite, silica fume and fly ash. *Construction and Building Materials*, *44*, 175–184. https://doi.org/10.1016/j.conbuildmat.2013.02.069

Saini, G., & Vattipalli, U. (2020). Assessing properties of alkali activated GGBS based self-compacting geopolymer concrete using nano-silica. *Case Studies in Construction Materials*,

12, e00352. https://doi.org/10.1016/j.cscm.2020.e00352

Schmidhuber, J. (2015). Deep Learning in neural networks: An overview. In *Neural Networks* (Vol. 61, pp. 85–117). Elsevier Ltd. https://doi.org/10.1016/j.neunet.2014.09.003

Serraye, M., Kenai, S., & Boukhatem, B. (2021). Prediction of compressive strength of self-compacting concrete (SCC) with silica fume using neural networks models. *Civil Engineering Journal (Iran)*, *7*(1), 118–139. https://doi.org/10.28991/cej-2021-03091642

Siddique, R. (2011). Properties of self-compacting concrete containing class F fly ash. *Materials and Design*, *32*(3), 1501–1507. https://doi.org/10.1016/j.matdes.2010.08.043

Siddique, R., Aggarwal, P., & Aggarwal, Y. (2011). Prediction of compressive strength of self-compacting concrete containing bottom ash using artificial neural networks. *Advances in Engineering Software*, *42*(10), 780–786. https://doi.org/10.1016/j.advengsoft.2011.05.016

Siddique, R., Aggarwal, P., Aggarwal, Y., Gupta, S. M., Siddique, R., Aggarwal, P., Aggarwal, Y., & Gupta, S. M. (2008). Modeling properties of self-compacting concrete: support vector machines approach. *Computers and Concrete*, *5*(5), 461. https://doi.org/10.12989/CAC.2008.5.5.461

Taylor, J. G. (Ed.). (1992). *Neural Network Applications*. https://doi.org/10.1007/978-1-4471-2003-2

Turk, K., Karatas, M., & Gonen, T. (2013a). Effect of Fly Ash and Silica Fume on compressive strength, sorptivity and carbonation of SCC. *KSCE Journal of Civil Engineering*, *17*(1), 202–209. https://doi.org/10.1007/s12205-013-1680-3

Turk, K., Karatas, M., & Gonen, T. (2013b). Effect of Fly Ash and Silica Fume on compressive strength, sorptivity and carbonation of SCC. *KSCE Journal of Civil Engineering*, *17*(1), 202–209. https://doi.org/10.1007/s12205-013-1680-3

Uysal, M., & Tanyildizi, H. (2011). Predicting the core compressive strength of self-compacting concrete (SCC) mixtures with mineral additives using artificial neural network. *Construction and Building Materials*, *25*(11), 4105–4111. https://doi.org/10.1016/J.CONBUILDMAT.2010.11.108

Vandeput, N. (n.d.). *Forecast KPI: RMSE, MAE, MAPE & Bias | Towards Data Science*. Retrieved August 29, 2021, from https://towardsdatascience.com/forecast-kpi-rmse-mae-mape-bias-cdc5703d242d

Vivek, S. S., & Dhinakaran, G. (2017). Fresh and hardened properties of binary blend high strength self compacting concrete. *Engineering Science and Technology, an International Journal*, *20*(3), 1173–1179. https://doi.org/10.1016/j.jestch.2017.05.003

Wongkeo, W., Thongsanitgarn, P., Ngamjarurojana, A., & Chaipanich, A. (2014). Compressive strength and chloride resistance of self-compacting concrete containing high level fly ash and silica fume. *Materials and Design*, *64*, 261–269. https://doi.org/10.1016/j.matdes.2014.07.042

Yadollahi, M. M., Benli, A., & Demirboⅼa, R. (2015). Prediction of compressive strength of geopolymer composites using an artificial neural network. *Materials Research Innovations*, *19*(6), 453–458. https://doi.org/10.1179/1433075X15Y.0000000020

Ye, X. W., Jin, T., & Yun, C. B. (2019). A review on deep learning-based structural health monitoring of civil infrastructures. *Smart Structures and Systems*, *24*(5), 567. https://doi.org/10.12989/SSS.2019.24.5.567

Zhu, W., & Bartos, P. J. M. (2003). Permeation properties of self-compacting concrete. *Cement and Concrete Research*, *33*(6), 921–926. https://doi.org/10.1016/S0008-8846(02)01090-6

Appendix-I

Table A 1: Data Sources

W/B	C	FA	SF	FnA	CA	SP	VMA	Age	F'c	Author
0.33	500	0	0	984	656	6.5	0	28	65	(Sabet et al., 2013)
0.33	450	0	50	959	656	9.5	0	28	75.5	
0.33	400	0	100	935	656	12	0	28	79.5	
0.33	450	50	0	966	656	5.5	0	28	67	
0.33	400	100	0	948	656	4	0	28	80.5	
0.33	450	0	50	959	656	9.5	0	90	73	
0.33	400	0	100	935	656	12	0	90	79.5	
0.33	450	50	0	966	656	5.5	0	90	73	
0.33	400	100	0	948	656	4	0	90	79.5	
0.33	450	0	50	959	656	9.5	0	180	79.5	
0.33	400	0	100	935	656	12	0	180	87	
0.33	450	50	0	966	656	5.5	0	180	79.5	
0.33	400	100	0	948	656	4	0	180	87	
0.35	550	0	0	688	688	5.5	0	28	48	(Güneyisi et al., 2015)
0.35	467.5	82.5	0	677	677	5.3	0	28	45	
0.35	385	165	0	665	665	5.3	0	28	42	
0.35	522.5	0	27.5	684	684	6.4	0	28	53	
0.35	495	0	55	680	680	6.4	0	28	54	
0.35	440	82.5	27.5	670	670	6.2	0	28	47	
0.35	412.5	82.5	55	669	668	6.2	0	28	47	
0.35	357.5	165	27.5	661	661	5.6	0	28	43	
0.35	330	165	55	657	657	5.6	0	28	43	
0.30	600	0	0	1084	595	7.14	0	7	79.3	(Wongkeo et al., 2014)
0.30	300	300	0	958	595	1.5	0	7	48.9	
0.30	240	360	0	933	595	1.02	0	7	37.9	
0.30	180	420	0	908	595	0.72	0	7	28.9	
0.30	570	0	30	1072	595	7.98	0	7	81.6	
0.30	540	0	60	1059	595	8.58	0	7	84.5	
0.30	300	270	30	958	595	2.22	0	7	56	
0.30	240	330	30	933	595	1.8	0	7	49.1	
0.30	180	390	30	908	595	1.2	0	7	39.5	
0.30	300	240	60	958	595	3.6	0	7	66.1	
0.30	240	300	60	933	595	2.88	0	7	55.1	
0.30	180	360	60	908	595	2.28	0	7	46.9	

W/B	C	FA	SF	FnA	CA	SP	VMA	Age	F'c	Author
0.30	600	0	0	1084	595	7.14	0	28	84	
0.30	300	300	0	958	595	1.5	0	28	66.4	
0.30	240	360	0	933	595	1.02	0	28	58	
0.30	180	420	0	908	595	0.72	0	28	45.6	
0.30	570	0	30	1072	595	7.98	0	28	95.3	
0.30	540	0	60	1059	595	8.58	0	28	100.5	
0.30	300	270	30	958	595	2.22	0	28	75.2	
0.30	240	330	30	933	595	1.8	0	28	63.4	
0.30	180	390	30	908	595	1.2	0	28	52.7	
0.30	300	240	60	958	595	3.6	0	28	85.2	
0.30	240	300	60	933	595	2.88	0	28	73.6	
0.30	180	360	60	908	595	2.28	0	28	61.2	
0.30	600	0	0	1084	595	7.14	0	90	88.3	
0.30	300	300	0	958	595	1.5	0	90	81.1	
0.30	240	360	0	933	595	1.02	0	90	68.8	
0.30	180	420	0	908	595	0.72	0	90	55.2	
0.30	570	0	30	1072	595	7.98	0	90	99	
0.30	540	0	60	1059	595	8.58	0	90	106.6	
0.30	300	270	30	958	595	2.22	0	90	89.5	
0.30	240	330	30	933	595	1.8	0	90	74.1	
0.30	180	390	30	908	595	1.2	0	90	61.6	
0.30	300	240	60	958	595	3.6	0	90	96.6	
0.30	240	300	60	933	595	2.88	0	90	85.9	
0.30	180	360	60	908	595	2.28	0	90	80.6	
0.35	514	0	0	1131	621	7.71	0	7	75.2	
0.35	257	257	0	1023	621	1.3364	0	7	44.6	
0.35	206	309	0	1001	621	0.9785	0	7	33.7	
0.35	154	360	0	980	621	0.6682	0	7	23.6	
0.35	489	0	26	1120	621	8.24	0	7	77.6	
0.35	463	0	51	1110	621	8.995	0	7	81.2	
0.35	257	231	26	1023	621	2.056	0	7	50.4	
0.35	206	283	26	1001	621	1.648	0	7	44	
0.35	154	334	26	980	621	1.1308	0	7	33.5	
0.35	257	206	51	1023	621	3.1868	0	7	53.1	
0.35	206	257	51	1001	621	2.57	0	7	48.2	
0.35	154	309	51	980	621	2.056	0	7	40.5	
0.35	514	0	0	1131	621	7.71	0	28	83	
0.35	257	257	0	1023	621	1.3364	0	28	59.2	

W/B	C	FA	SF	FnA	CA	SP	VMA	Age	F'c	Author
0.35	206	309	0	1001	621	0.9785	0	28	52.6	
0.35	154	360	0	980	621	0.6682	0	28	39.8	
0.35	489	0	26	1120	621	8.24	0	28	85.3	
0.35	463	0	51	1110	621	8.995	0	28	91.6	
0.35	257	231	26	1023	621	2.056	0	28	68.4	
0.35	206	283	26	1001	621	1.648	0	28	57.4	
0.35	154	334	26	980	621	1.1308	0	28	45.9	
0.35	257	206	51	1023	621	3.1868	0	28	75.4	
0.35	206	257	51	1001	621	2.57	0	28	64.7	
0.35	154	309	51	980	621	2.056	0	28	51.1	
0.35	514	0	0	1131	621	7.71	0	90	85.4	
0.35	257	257	0	1023	621	1.3364	0	90	70.9	
0.35	206	309	0	1001	621	0.9785	0	90	64	
0.35	154	360	0	980	621	0.6682	0	90	50.1	
0.35	489	0	26	1120	621	8.24	0	90	90.9	
0.35	463	0	51	1110	621	8.995	0	90	100.4	
0.35	257	231	26	1023	621	2.056	0	90	82.5	
0.35	206	283	26	1001	621	1.648	0	90	69.6	
0.35	154	334	26	980	621	1.1308	0	90	57.3	
0.35	257	206	51	1023	621	3.1868	0	90	86.6	
0.35	206	257	51	1001	621	2.57	0	90	78.9	
0.35	154	309	51	980	621	2.056	0	90	70.4	
0.40	450	0	0	1166	640	8.1	0	7	65.6	
0.40	225	225	0	1072	640	1.17	0	7	25.7	
0.40	180	270	0	1053	640	0.945	0	7	21.2	
0.40	135	315	0	1034	640	0.585	0	7	17.7	
0.40	428	0	23	1157	640	8.569	0	7	65.8	
0.40	405	0	45	1147	640	9.45	0	7	69.7	
0.40	225	203	23	1072	640	1.9393	0	7	32.1	
0.40	180	248	23	1053	640	1.5334	0	7	29.8	
0.40	135	293	23	1034	640	1.2628	0	7	18.2	
0.40	225	180	45	1072	640	2.88	0	7	36.5	
0.40	180	225	45	1053	640	2.34	0	7	37	
0.40	135	270	45	1034	640	2.07	0	7	22.9	
0.40	450	0	0	1166	640	8.1	0	28	72.4	
0.40	225	225	0	1072	640	1.17	0	28	41.9	
0.40	180	270	0	1053	640	0.945	0	28	35.7	
0.40	135	315	0	1034	640	0.585	0	28	31.7	

W/B	C	FA	SF	FnA	CA	SP	VMA	Age	F'c	Author
0.40	428	0	23	1157	640	8.569	0	28	75.3	
0.40	405	0	45	1147	640	9.45	0	28	79	
0.40	225	203	23	1072	640	1.9393	0	28	51.5	
0.40	180	248	23	1053	640	1.5334	0	28	39.2	
0.40	135	293	23	1034	640	1.2628	0	28	28.2	
0.40	225	180	45	1072	640	2.88	0	28	60.3	
0.40	180	225	45	1053	640	2.34	0	28	49.1	
0.40	135	270	45	1034	640	2.07	0	28	33.1	
0.40	450	0	0	1166	640	8.1	0	90	80.4	
0.40	225	225	0	1072	640	1.17	0	90	53.1	
0.40	180	270	0	1053	640	0.945	0	90	48	
0.40	135	315	0	1034	640	0.585	0	90	41.8	
0.40	428	0	23	1157	640	8.569	0	90	82.4	
0.40	405	0	45	1147	640	9.45	0	90	86.1	
0.40	225	203	23	1072	640	1.9393	0	90	64	
0.40	180	248	23	1053	640	1.5334	0	90	51.3	
0.40	135	293	23	1034	640	1.2628	0	90	42.3	
0.40	225	180	45	1072	640	2.88	0	90	71.4	
0.40	180	225	45	1053	640	2.34	0	90	63.8	
0.40	135	270	45	1034	640	2.07	0	90	52.5	
0.32	550	0	0	728	935	8.43	0	28	80.9	(Güneyisi et al.,
0.32	440	110	0	714	917	7.43	0	28	69.8	2010)
0.32	330	220	0	700	899	7.43	0	28	60.9	
0.32	220	330	0	686	881	6.67	0	28	47.5	
0.32	522.5	0	27.5	724	930	9.56	0	28	80.4	
0.32	495	0	55	720	925	10.67	0	28	85.7	
0.32	467.5	0	82.5	716	920	12	0	28	84.4	
0.32	440	82.5	27.5	713	916	8.22	0	28	79.2	
0.32	330	165	55	699	898	9.11	0	28	67.2	
0.32	220	247.5	82.5	685	880	8.89	0	28	60	
0.44	450	0	0	826	868	3.5	0	28	61.5	
0.44	360	90	0	813	855	3.2	0	28	52.1	
0.44	270	180	0	801	842	2.96	0	28	44.7	
0.44	180	270	0	788	829	3	0	28	30.3	
0.44	427.5	0	22.5	823	865	4.88	0	28	60.7	
0.44	405	0	45	819	861	5.2	0	28	58.5	
0.44	382.5	0	67.5	816	858	7.76	0	28	71.1	
0.44	360	67.5	22.5	813	855	4.24	0	28	61.5	

W/B	C	FA	SF	FnA	CA	SP	VMA	Age	F'c	Author
0.44	270	135	45	801	841	4.52	0	28	46.9	
0.44	180	202.5	67.5	788	828	4.82	0	28	37.4	
0.32	550	0	0	728	935	8.43	0	90	91.1	
0.32	440	110	0	714	917	7.43	0	90	84.4	
0.32	330	220	0	700	899	7.43	0	90	77.9	
0.32	220	330	0	686	881	6.67	0	90	64.8	
0.32	522.5	0	27.5	724	930	9.56	0	90	91.8	
0.32	495	0	55	720	925	10.67	0	90	99.2	
0.32	467.5	0	82.5	716	920	12	0	90	96.7	
0.32	440	82.5	27.5	713	916	8.22	0	90	86.3	
0.32	330	165	55	699	898	9.11	0	90	80.1	
0.32	220	247.5	82.5	685	880	8.89	0	90	68.3	
0.44	450	0	0	826	868	3.5	0	90	73.6	
0.44	360	90	0	813	855	3.2	0	90	68	
0.44	270	180	0	801	842	2.96	0	90	60.3	
0.44	180	270	0	788	829	3	0	90	42.5	
0.44	427.5	0	22.5	823	865	4.88	0	90	71.2	
0.44	405	0	45	819	861	5.2	0	90	76.1	
0.44	382.5	0	67.5	816	858	7.76	0	90	74.8	
0.44	360	67.5	22.5	813	855	4.24	0	90	67.2	
0.44	270	135	45	801	841	4.52	0	90	57.6	
0.44	180	202.5	67.5	788	828	4.82	0	90	44.8	
0.44	450	0	0	826	868	3.5	0	90	73.6	(Gesoğlu et al., 2009)
0.44	360	90	0	813	855	3.2	0	90	68	
0.44	270	180	0	801	842	2.9	0	90	60.3	
0.44	180	270	0	788	829	3	0	90	42.5	
0.44	428	0	22.5	823	865	4.9	0	90	71.2	
0.44	405	0	45	819	861	5.2	0	90	76.1	
0.44	383	0	67.5	816	858	7.8	0	90	74.8	
0.44	360	67.5	22.5	813	855	4.2	0	90	67.2	
0.44	270	135	45	801	841	4.5	0	90	57.6	
0.44	180	202.5	67.5	788	828	4.8	0	90	44.9	
0.32	550	0	0	728	935	8.43	0	28	80.9	(Gesoğlu & Özbay, 2007)
0.32	440	110	0	714	917	7.43	0	28	69.8	
0.32	330	220	0	700	899	7.43	0	28	60.9	
0.32	220	330	0	686	881	6.67	0	28	47.5	
0.32	522.5	0	27.5	724	930	9.56	0	28	80.3	
0.32	495	0	55	720	925	10.67	0	28	85.6	

W/B	C	FA	SF	FnA	CA	SP	VMA	Age	F'c	Author
0.32	467.5	0	82.5	716	920	12	0	28	84.4	
0.32	440	82.5	27.5	713	916	8.22	0	28	79.2	
0.32	330	165	55	699	898	9.11	0	28	67.2	
0.32	220	247.5	82.5	685	880	8.89	0	28	59.9	
0.38	444	0	0	1010	777	4.44	0	28	53.8	(Behfarnia &
0.38	421.8	0	22.2	1002	777	5.328	0	28	63	Farshadfar, 2013)
0.38	399.6	0	44.4	994	777	6.66	0	28	63.8	
0.38	377.8	0	66.2	986	777	6.66	0	28	72.1	
0.38	444	0	0	1010	777	4.44	0	90	57	
0.38	421.8	0	22.2	1002	777	5.328	0	90	68	
0.38	399.6	0	44.4	994	777	6.66	0	90	67	
0.38	377.8	0	66.2	986	777	6.66	0	90	71.5	
0.35	500	0	0	967	694	8	0	28	78.5	(Bingöl &
0.35	475	0	25	958	687	8	0	28	78.5	Tohumcu, 2013)
0.35	450	0	50	954	685	9	0	28	82.5	
0.35	425	0	75	948	681	10	0	28	87	
0.35	375	125	0	938	673	7.5	0	28	61.5	
0.35	300	200	0	923	663	7.5	0	28	55	
0.35	225	275	0	908	652	7.5	0	28	43	
0.40	600	0	0	810	660	13.8	0.9	7	35	(Vivek &
0.40	570	0	30	810	660	13.8	0.9	7	34	Dhinakaran, 2017)
0.40	540	0	60	810	660	13.8	0.9	7	32	
0.40	510	0	90	810	660	13.8	0.9	7	31	
0.40	600	0	0	810	660	13.8	0.9	28	63	
0.40	570	0	30	810	660	13.8	0.9	28	60.1	
0.40	540	0	60	810	660	13.8	0.9	28	58.1	
0.40	510	0	90	810	660	13.8	0.9	28	55.3	
0.40	480	0	120	810	660	13.8	0.9	28	51.38	
0.40	450	0	150	810	660	13.8	0.9	28	45.08	
0.45	400	0	0	793	1000	1.3	0	7	46	(Khodabakhshian et
0.45	390	0	10	790.7	1000	1.45	0	7	48	al., 2018)
0.45	380	0	20	788.4	1000	1.45	0	7	48	
0.45	360	0	40	783.8	1000	1.6	0	7	53	
0.45	400	0	0	793	1000	1.3	0	28	52	
0.45	390	0	10	790.7	1000	1.45	0	28	59	
0.45	380	0	20	788.4	1000	1.45	0	28	60	
0.45	360	0	40	783.8	1000	1.6	0	28	66	
0.45	400	0	0	793	1000	1.3	0	180	62	

W/B	C	FA	SF	FnA	CA	SP	VMA	Age	F'c	Author
0.45	390	0	10	790.7	1000	1.45	0	180	71	
0.45	380	0	20	788.4	1000	1.45	0	180	73	
0.45	360	0	40	783.8	1000	1.6	0	180	77	
0.36	500	0	0	893	735	7	0	7	39	(Turk et al., 2013b)
0.39	375	125	0	910	735	6.75	0	7	30	
0.38	350	150	0	910	735	6.75	0	7	33	
0.38	325	175	0	910	735	6.75	0	7	29.5	
0.38	300	200	0	910	735	6.75	0	7	28	
0.36	427.5	0	22.5	990	735	8	0	7	43.9	
0.38	405	0	45	990	735	8	0	7	47	
0.40	382.5	0	67.5	990	735	8	0	7	41	
0.40	360	0	90	990	735	8	0	7	40.5	
0.36	500	0	0	893	735	7	0	28	57.5	
0.39	375	125	0	910	735	6.75	0	28	50	
0.38	350	150	0	910	735	6.75	0	28	45	
0.38	325	175	0	910	735	6.75	0	28	43	
0.38	300	200	0	910	735	6.75	0	28	45	
0.36	427.5	0	22.5	990	735	8	0	28	58	
0.38	405	0	45	990	735	8	0	28	62.8	
0.40	382.5	0	67.5	990	735	8	0	28	68	
0.40	360	0	90	990	735	8	0	28	66.4	
0.37	360	0	40	1069	766	3.45	0	7	38	(Gholhaki et al., 2018)
0.37	320	0	80	1062	761	5.37	0	7	40	
0.37	360	40	0	1070	767	2.68	0	7	39.5	
0.37	320	80	0	1065	764	2.11	0	7	41	
0.37	400	0	0	1085	778	5.75	0	28	38	
0.37	360	0	40	1069	766	3.45	0	28	54	
0.37	320	0	80	1062	761	5.37	0	28	57.5	
0.37	360	40	0	1070	767	2.68	0	28	48	
0.37	320	80	0	1065	764	2.11	0	28	52	
0.44	350	0	35	960	920	2.76	0	7	21.1	(Faez et al., 2020)
0.44	350	0	35	960	920	2.76	0	28	26.1	
0.44	350	0	35	960	920	2.76	0	90	29.3	
0.33	550	0	0	970	722	7.7	0	7	38	(Choudhary et al., 2020)
0.33	522.5	0	27.5	970	722	8.25	0	7	44	
0.33	440	82.5	27.5	970	722	3.3	0	7	47.5	
0.33	385	137.5	27.5	970	722	1.65	0	7	42.5	
0.33	330	192.5	27.5	970	722	1.21	0	7	37.5	

W/B	C	FA	SF	FnA	CA	SP	VMA	Age	F'c	Author
0.33	550	0	0	970	722	7.7	0	28	55.5	
0.33	522.5	0	27.5	970	722	8.25	0	28	58	
0.33	440	82.5	27.5	970	722	3.3	0	28	51	
0.33	385	137.5	27.5	970	722	1.65	0	28	54	
0.33	330	192.5	27.5	970	722	1.21	0	28	45	
0.33	550	0	0	970	722	7.7	0	90	57	
0.33	522.5	0	27.5	970	722	8.25	0	90	60	
0.33	440	82.5	27.5	970	722	3.3	0	90	60	
0.33	385	137.5	27.5	970	722	1.65	0	90	59	
0.33	330	192.5	27.5	970	722	1.21	0	90	56	
0.39	220	180	0	916	900	1.4	0	28	49	(Patel et al., 2004)
0.39	220	180	0	916	900	1.4	0	28	49	
0.39	160	240	0	886	900	1.4	0	28	44	
0.34	198	232	0	874	900	0.86	0	28	46	
0.39	248	203	0	808	900	1.575	0	28	50	
0.39	220	180	0	916	900	1.4	0	28	49	
0.43	237	133	0	960	900	1.85	0	28	46	
0.39	280	120	0	946	900	1.4	0	28	45	
0.43	170	200	0	930	900	0.74	0	28	31	
0.39	220	180	0	916	900	1.4	0	28	47	
0.36	198	232	0	872	900	2.15	0	28	52	
0.39	220	180	0	916	900	1.4	0	28	45	
0.43	170	200	0	928	900	1.85	0	28	33	
0.38	250	257	0	787	853	2.42	0	7	34	(Bui et al., 2002)
0.36	427	115	0	779	844	2.76	0	7	52.1	
0.35	327	173	0	902	803	4.42	0	7	50.2	
0.35	380	145	0	788	854	2.2	0	7	53.2	
0.33	350	186	0	786	851	2.4	0	7	51.1	
0.35	380	192	0	931	621	2.27	0	7	45.7	
0.41	350	162	0	768	840	1.94	0	28	51.7	
0.38	250	257	0	787	853	2.42	0	28	51.5	
0.36	427	115	0	779	844	2.76	0	28	59.4	
0.35	327	173	0	902	803	4.42	0	28	61.6	
0.35	380	145	0	788	854	2.2	0	28	73.5	
0.33	350	186	0	786	851	2.4	0	28	70.4	
0.35	380	192	0	931	621	2.27	0	28	67.8	
0.41	465	85	0	910	590	10.73	0	7	29.55	(Siddique, 2011)
0.41	440	110	0	910	590	11.01	0	7	27.99	

W/B	C	FA	SF	FnA	CA	SP	VMA	Age	F'c	Author
0.42	415	135	0	910	590	9.91	0	7	25.52	
0.43	385	165	0	910	590	9.91	0	7	23.98	
0.44	355	195	0	910	590	9.91	0	7	22.78	
0.41	465	85	0	910	590	10.73	0	28	35.19	
0.41	440	110	0	910	590	11.01	0	28	33.15	
0.42	415	135	0	910	590	9.91	0	28	31.47	
0.43	385	165	0	910	590	9.91	0	28	30.66	
0.44	355	195	0	910	590	9.91	0	28	29.62	
0.41	465	85	0	910	590	10.73	0	90	58.99	
0.41	440	110	0	910	590	11.01	0	90	52.86	
0.42	415	135	0	910	590	9.91	0	90	43.77	
0.43	385	165	0	910	590	9.91	0	90	41.96	
0.44	355	195	0	910	590	9.91	0	90	40.88	
0.45	530	0	0	768	668	0.86	0.082	28	30	(Dhiyaneshwaran et al., 2013)
0.45	477	53	0	768	668	0.86	0.082	28	32.2	
0.45	424	106	0	768	668	0.86	0.082	28	37.9	
0.45	371	159	0	768	668	0.86	0.082	28	41.4	
0.45	318	212	0	768	668	0.86	0.082	28	37.2	
0.45	265	265	0	768	668	0.86	0.082	28	35.9	
0.45	530	0	0	768	668	0.86	0.082	7	20	
0.45	477	53	0	768	668	0.86	0.082	7	23.4	
0.45	424	106	0	768	668	0.86	0.082	7	26.7	
0.45	371	159	0	768	668	0.86	0.082	7	29.16	
0.45	318	212	0	768	668	0.86	0.082	7	28.6	
0.45	265	265	0	768	668	0.86	0.082	7	27.2	
0.35	500	0	0	967	694	8	0	28	78.6	(Bingöl & Tohumcu, 2013)
0.35	475	0	25	958	687	8	0	28	78.6	
0.35	450	0	50	954	685	9	0	28	82	
0.35	425	0	75	948	681	10	0	28	88	
0.35	375	125	0	938	673	7.5	0	28	62.5	
0.35	300	200	0	923	663	7.5	0	28	55	
0.35	225	275	0	908	652	7.5	0	28	42.7	
0.40	480	0	0	890	810	13.3	0	28	52	(Prajapati Krishnapal, 2013)
0.40	432	48	0	890	810	9.9	0	28	46	
0.40	384	96	0	890	810	9.68	0	28	42	
0.40	336	144	0	890	810	9.4	0	28	40	
0.45	450	0	0	890	810	9.25	0	28	50	
0.45	405	45	0	890	810	8.2	0	28	45	

W/B	C	FA	SF	FnA	CA	SP	VMA	Age	F'c	Author
0.45	360	90	0	890	810	6.4	0	28	41	
0.45	315	135	0	890	810	4.8	0	28	39	
0.40	480	0	0	890	810	13.3	0	7	36	
0.40	432	48	0	890	810	9.9	0	7	33	
0.40	384	96	0	890	810	9.68	0	7	26	
0.40	336	144	0	890	810	9.4	0	7	24	
0.45	450	0	0	890	810	9.25	0	7	32	
0.45	405	45	0	890	810	8.2	0	7	31	
0.45	360	90	0	890	810	6.4	0	7	24	
0.45	315	135	0	890	810	4.8	0	7	22	

W/B: Water/binder ratio
C: Cement
FA: Fly ash
SF: Silica fume
FnA: Fine aggregates
CA: Coarse aggregates
SP: Superplasticizer
VMA: Viscosity modifying agent
F'c: Compressive strength

Appendix-II

Table B 1: Statistical indexes of the investigated BPNN models

SL No.	BPNN Model	Dataset	R^2	RMSE
1	9-5-1	Training	0.9663	3.4842503
		Validation	0.9465	4.5022217
		Test	0.9241	5.2773099
2	9-6-1	Training	0.9592	3.8600518
		Validation	0.9245	5.5569776
		Test	0.9305	4.9020404
3	9-7-1	Training	0.9629	3.6945906
		Validation	0.9518	4.2906876
		Test	0.9423	4.6733286
4	9-8-1	Training	0.9763	2.9444864
		Validation	0.9195	5.6603887
		Test	0.8934	5.9312731
5	9-9-1	Training	0.9734	3.0413813
		Validation	0.9359	4.9779514
		Test	0.8868	7.1888803
6	9-10-1	Training	0.9839	2.3065125
		Validation	0.9364	4.9081565
		Test	0.9628	3.6619667
7	9-11-1	Training	0.9821	2.6019224
		Validation	0.9268	5.745433
		Test	0.8964	5.1029403
8	9-12-1	Training	0.9628	3.7296112
		Validation	0.9048	5.7628118
		Test	0.8898	6.6030296
9	9-13-1	Training	0.9825	2.521904
		Validation	0.8694	6.4660653
		Test	0.9349	5.1097945
10	9-14-1	Training	0.9750	2.9171904
		Validation	0.9328	4.6968074
		Test	0.9397	5.7297469

SL No.	BPNN Model	Dataset	R^2	RMSE
11	9-15-1	Training	0.9734	3.0430248
		Validation	0.9181	5.097058
		Test	0.9428	5.2886671
12	9-16-1	Training	0.9324	5.052722
		Validation	0.9164	5.3366656
		Test	0.8853	7.2518963
13	9-17-1	Training	0.9864	2.2135944
		Validation	0.9510	4.2614552
		Test	0.9274	4.8155997
14	9-18-1	Training	0.9677	3.4058773
		Validation	0.9057	5.937171
		Test	0.9475	4.9507575
15	9-19-1	Training	0.9857	2.2956481
		Validation	0.9214	5.884726
		Test	0.9044	5.7489129
16	9-20-1	Training	0.9872	2.2825424
		Validation	0.9149	5.6665686
		Test	0.8703	6.9152006
17	9-21-1	Training	0.9847	2.3086793
		Validation	0.9510	4.9638695
		Test	0.9407	4.3185646
18	9-22-1	Training	0.9896	1.9595918
		Validation	0.9107	5.2038447
		Test	0.9390	5.0566788
19	9-23-1	Training	0.9942	1.43527
		Validation	0.9218	5.2801515
		Test	0.9063	5.7576037

BPNN: Back propagation neural network
R: Correlation coefficient
RMSE: Root mean square error